Knowledge and Information Systems
https://doi.org/10.1007/s10115-025-02561-9

RESEARCH

Multi-strategies improved coati optimization algorithm and performance analysis

Chunqing Li[1] · Zhongmin Wang[2] · Jun Yu[3] · Mahmoud Abdel-Salam[4] · Essam H. Houssein[5,6] · Rui Zhong[7]

Received: 15 January 2025 / Revised: 24 June 2025 / Accepted: 23 July 2025

Abstract
Coati optimization algorithm (COA) as a novel swarm intelligence approach has the advantages of fast convergence speed and high accuracy, but it also has shortages of easy premature and unbalanced searchability. To handle these problems, this paper presents an efficient Multi-Strategies Improved COA (MSICOA), which integrates three strategies: (1) the nonlinear inertia weight factor to control the behaviors of coatis, (2) the Harris Hawk besieging mechanism from Harris Hawks Optimization (HHO) to balance the ability of coatis between local and global searchability, and (3) the sparrow vigilant mechanism in the Sparrow Search Algorithm (SSA) to improve the vigilance ability of the coatis to search in the search domain and accelerate the convergence speed. Computational complexity analysis confirms that the proposed MSICOA has identical computational complexity with COA theoretically. Comprehensive numerical experiments in CEC2017 and CEC2020 against twelve well-known optimizers demonstrate the superiority of MSICOA, and ablation experiments validate the independent contribution of integrated three strategies. Finally, MSICOA is employed to solve six engineering problems, and the experimental results show that the proposed MSICOA has remarkable convergence accuracy, robustness, and practicality. The source code of this research can be downloaded at https://github.com/RuiZhong961230/MSICOA.

Keywords Metaheuristic algorithm · Coati optimization algorithm · Nonlinear inertia weight · Harris Hawk besieging mechanism · Sparrow vigilant mechanism

1 Introduction

Swarm intelligence optimization algorithms are inspired by the evolutionarily developed behaviors and survival strategies of biological groups, which utilize collective behavior for problem-solving [1–3]. These algorithms address complex optimization challenges, including high-dimensional, multi-constraint, and nonlinear problems, by simulating the behaviors and cooperative information-sharing of biological systems [4–6]. Classic swarm intelligence optimization algorithms, such as particle swarm optimization (PSO) [7], ant colony optimization (ACO) [8], and genetic algorithm (GA) [9], have laid the groundwork for this field. However, they exhibit limitations like slow convergence speed, low solution accuracy, and higher computational demands, particularly when applied to complex problems. To over-

Extended author information available on the last page of the article

Published online: 22 August 2025

come these drawbacks, researchers have developed numerous enhanced and more effective algorithms. For instance, the osprey optimization algorithm (OOA) [10] simulates osprey's strategic hunting behavior, while the pelicans optimization algorithm (POA) [11], proposed by Pavel et al., models pelican prey capture strategies. The artificial gorilla troop optimization (GTO) algorithm [12], introduced by Abdollahzadeh et al., draws on gorillas' collective social behaviors, and the dung beetle optimization (DBO) algorithm [13], introduced by Xue et al., incorporates the unique foraging and reproductive behaviors of dung beetles, such as ball rolling and resource stealing. These and other recently developed algorithms have demonstrated great promise and adaptability in diverse applications, including lithium-ion battery model parameter estimation, industrial IoT environment monitoring, and 3D UAV path planning [14–18]. The rise of these algorithms has fueled advancements in addressing real-world, large-scale optimization tasks across various fields. Through ongoing research, improved algorithms continue to emerge, enabling swarm intelligence approaches to maintain an expanding influence in scientific and engineering domains [19–22].

Dehghani et al. [23] introduced the Coati Optimization Algorithm (COA) in 2023, inspired by the natural hunting and evasion behaviors of coatis. COA exhibits key characteristics of randomness and population diversity, which enables it well suited for a broad spectrum of optimization tasks, including continuous, discrete, and multi-objective problems [24–26]. Its ability to balance exploration and exploitation allows it to effectively navigate and search complex solution spaces, often achieving better performance than many traditional algorithms. In this study, we propose a Multi-Strategies Improved COA (MSICOA) that enhances the efficiency and robustness of COA by introducing three efficient mechanisms:

- Nonlinear Inertia Weight Factor: During the exploration phase, a nonlinear inertia weight factor is integrated into the coatis positioned in the tree area to fine-tune the correlation and information among coatis.
- Harris Hawk Besieging Mechanism: Inspired by the Harris Hawks Optimization (HHO), this mechanism is incorporated for under-tree coatis to strengthen their attack dynamics and improve convergence speed.
- Sparrow Vigilant Mechanism: Derived from the Sparrow Search Algorithm (SSA), this vigilance mechanism improves the later-stage alertness of MSICOA and enables the coatis to refine their search within the feasible range and avoid local optima traps.

A comprehensive time complexity analysis reveals that the modifications in MSICOA do not cause significant computational complexity increases compared with the original COA. Additionally, the effectiveness of the proposed MSICOA is evaluated in CEC2017 and CEC2020 benchmarks, which demonstrate superior convergence speed, accuracy, and global optimization performance of MSICOA compared to twelve well-known optimizers. Furthermore, the ablation experiments are conducted to validate the contribution of the integrated strategies independently. Moreover, the performance of MSICOA is evaluated across six real-world engineering optimization problems, which practically confirms its applicability and strength in tackling practical engineering challenges. This study highlights MSICOA as a powerful and versatile tool in metaheuristic algorithms and provides significant improvements in convergence and solution accuracy across a variety of complex problem domains. Briefly, the contributions of this paper are summarized as follows.

- We propose an efficient Multi-Strategies Improved Coati Optimization Algorithm (MSICOA) by introducing three strategies: (1) nonlinear inertia weight factor, (2) Harris Hawk besieging mechanism, and (3) sparrow vigilant mechanism.
- The nonlinear inertia weight factor aims to fine-tune the correlation and information among coatis. The Harris Hawk besieging mechanism strengthens the attack dynamics

Fig. 1 Coatis in nature. **a** Coati in the tree. **b** Coati in the ground

of coatis to further improve convergence speed, and the sparrow vigilant mechanism refines the searchability in the large stage of optimization.
- Comprehensive numerical experiments in high-dimensional CEC2017 and low-dimensional CEC2020 benchmarks against state-of-the-art optimizers confirm the competitiveness of the proposed MSICOA.
- Ablation experiments are conducted to demonstrate the contribution of integrated strategies independently.

The rest of this paper is organized as follows: Sect. 2 introduces the related works including COA and the literature review of its developments. Section 3 details the proposed MSICOA, and the numerical experiments in CEC benchmarks are conducted in Sect. 4. The application of MSICOA in engineering problems is presented in Sect. 5. Finally, Sect. 6 concludes this paper.

2 Related works

This section presents the related works of this paper. Section 2.1 details the architecture of COA, while a brief literature review of COA is presented in Sect. 2.2.

2.1 Coati optimization algorithm

COA is inspired by the distinct behavioral patterns of coatis, specifically their behaviors of attacking prey, cooperative hunting, and evading predators. Figure 1[1] presents coatis in nature. These behaviors exhibit a unique blend of coordination, adaptability, and agility, which allows coatis to explore and exploit their environment effectively.

In COA, each coati is treated as a search individual within the search domain. The spatial position of each coati represents a set of decision variables corresponding to a possible solution to the optimization problem. In the initialization phase, COA assigns each coati a

[1] Images are downloaded from https://pixabay.com/ as copyright-free images.
(a) https://pixabay.com/photos/coati-wildlife-zoo-berlin-1278557/.
(b) https://pixabay.com/photos/coati-furry-curly-tail-curious-856743/.

random position within the defined boundaries of the search space, as formulated in Eq. (1).

$$X = \begin{bmatrix} \boldsymbol{x}_1 \\ \boldsymbol{x}_2 \\ \boldsymbol{x}_3 \\ \vdots \\ \boldsymbol{x}_N \end{bmatrix} = \begin{bmatrix} x_{11} & x_{12} & \cdots & x_{1D} \\ x_{21} & x_{22} & \cdots & x_{2D} \\ x_{31} & x_{32} & \cdots & x_{3D} \\ \vdots & \vdots & \ddots & \vdots \\ x_{N1} & x_{N2} & \cdots & x_{ND} \end{bmatrix}, \; x_{ij} = \quad r \cdot (ub_j - lb_j) + lb_j \tag{1}$$

where X denotes the coati population, $\boldsymbol{x}_i$ indicates the ith coati individual, and x_{ij} is the value in the jth dimension of the ith individual. N and D are the population size and the dimension size. This random initialization ensures a diverse distribution of candidate solutions in the search domain.

COA simulates the behavior of coatis with three key survival strategies observed in nature: attacking prey, cooperative hunting, and evading predators. These behaviors are partitioned into two primary operational phases of COA: the exploration phase and the exploitation phase. In the exploration phase, coatis encircle and approach their target iguana in a structured manner, where the movements of coatis are characterized by randomness and strategic distribution across the search space, which allows coatis to explore a wide range of potential solutions. In the exploitation phase, the behavior of fleeing from predators is modeled. A group of coatis performs calculated adjustments to their positions and refines solutions in regions that have demonstrated potential during the exploration phase. By alternating between these two phases, COA effectively balances exploration and exploitation and achieves both diversity in searching unknown areas and depth in refining promising solutions. In the following context, the exploration phase and the exploitation phase of COA are presented in detail.

2.1.1 Exploration phase: strategies for hunting and attacking iguanas

In the exploration phase of COA, coatis exhibit group-based strategies to hunt their prey, which is inspired by their natural cooperative tactics. Equation (2) formulates the random division of coatis.

$$X = \begin{cases} X_1 = \{\boldsymbol{x}_1, \boldsymbol{x}_2, \ldots, \boldsymbol{x}_{\lfloor \frac{n}{2} \rfloor}\} \\ X_2 = \{\boldsymbol{x}_{\lfloor \frac{n}{2} \rfloor + 1}, \boldsymbol{x}_{\lfloor \frac{n}{2} \rfloor + 2}, \ldots, \boldsymbol{x}_n\} \end{cases} \tag{2}$$

where $\lfloor \cdot \rfloor$ is the floor function. The coati swarm is randomly divided into two groups, and the first group climbs into the trees and strategically positions themselves to approach and intimidate the iguanas. This group encourages the iguanas to move or fall by climbing closer to the prey and pushing them into vulnerable positions. Equation (3) formulates this hunting behavior of coatis.

$$\boldsymbol{x}_{i,j}^{t+1} = \boldsymbol{x}_{i,j}^{t} + r \cdot \left(\boldsymbol{x}_{best,j} - I \cdot \boldsymbol{x}_{i,j}^{t} \right) \tag{3}$$

where r is randomly sampled in (0, 1), I is a random integer in $\{1, 2\}$, and $\boldsymbol{x}_{best,j}$ is the current best solution representing the iguanas. After the iguanas fall to the ground, the second group of coatis then actively attacks iguanas, which simulates a collective approach using Eq. (4).

$$\begin{aligned} \boldsymbol{x}_{rand,j} &= r \cdot (UB_j - LB_j) + LB_j \\ \boldsymbol{x}_{i,j}^{t+1} &= \begin{cases} \boldsymbol{x}_{i,j}^{t} + r \cdot (\boldsymbol{x}_{rand,j} - I \cdot \boldsymbol{x}_{i,j}^{t}), & \text{if } f(\boldsymbol{x}_{rand}) < f(\boldsymbol{x}_i^t) \\ \boldsymbol{x}_{i,j}^{t} + r \cdot (\boldsymbol{x}_{i,j}^{t} - X_{rand,j}), & \text{otherwise} \end{cases} \end{aligned} \tag{4}$$

where $\boldsymbol{x}_{rand}$ denotes the position of the iguanas that fall to the ground. Throughout the exploration phase, coatis continuously adjust their positions based on the location of the iguanas, where the iguana's position serves as a focal point, guiding the movements of coatis to the optimal solution.

2.1.2 Exploitation phase: escape from predators

In this stage of COA, the position update mechanism is designed to mimic the coatis' natural behavior response when facing predators, an instinctive behavior that emphasizes quick, localized movement toward safety. This behavior formulated in Eq. (5) is activated within the COA to enhance its local search capability, which allows coatis to exploit promising areas and refine candidate solutions.

$$\begin{aligned} ub_j &= \frac{UB_j}{t}, lb_j = \frac{LB_j}{t} \\ \boldsymbol{x}_{i,j}^{t+1} &= \boldsymbol{x}_{i,j}^{t} + \theta \cdot (r \cdot (ub_j - lb_j) + lb_j) \end{aligned} \tag{5}$$

where $t = 1, 2, \ldots, T$ denotes the current iteration, and θ is a random number in $(-1, 1)$. This adaptive fleeing behavior strengthens the capability of COA in refining the coatis swarm and increases its precision in the final stages of the search, where small, targeted movements help identify optimal solutions with improved accuracy.

2.1.3 Elite selection mechanism

Like most swarm intelligence approaches, COA adopts the elite-based selection mechanism in Eq. (6) to ensure the survival of elite coati individuals.

$$\boldsymbol{x}_i^{t+1} = \begin{cases} \boldsymbol{x}_i^{t+1}, & \text{if } f(\boldsymbol{x}_i^{t+1}) < f(\boldsymbol{x}_i^{t}) \\ \boldsymbol{x}_i^{t}, & \text{otherwise} \end{cases} \tag{6}$$

In summary, the pseudocode of COA is presented in Algorithm 1.

Algorithm 1 COA [23]

Require: Population size: N, Dimension: D, Maximum iteration: T
Ensure: Optimum: $\boldsymbol{x}_{best}$
Initialize coati swarm using Eq. (1)
$t = 1$
while $t \leq T$ **do**
  Divide coati swarm into two groups using Eq. (2)
  ► **Exploration Phase**
  The previous group of coatis updates using Eq. (3)
  The later group of coatis updates using Eq. (4)
  Elite-based selection using Eq. (6)
  ► **Exploitation Phase**
  Coatis escape from predators using Eq. (5)
  Elite-based selection using Eq. (6)
  Record $\boldsymbol{x}_{best}$
end while
return $\boldsymbol{x}_{best}$

2.2 Literature review of COA

As a popular optimization approach, COA has attracted widespread attention from researchers. Zhang et al. [27] presented an improved COA named TNTWCOA, where the chaotic sequence mechanism is introduced for initializing coati positions to enhance the quality of the initial solutions. By incorporating chaos theory, the initialization avoids premature convergence to local optima and ensures a more diverse solution space. In the exploration phase, an adaptive parameter mechanism is integrated into the coati position update formula. This scheme dynamically adjusts the trade-off between local and global search capabilities and further improves the ability of TNTWCOA to effectively balance exploration and exploitation during optimization. To further refine the exploitation phase, an adaptive T-distribution mutation strategy is adopted. This strategy adds flexibility by tuning mutation rates based on the search stage, which fosters greater diversity in solutions and mitigates stagnation in local optima. Finally, TNTWCOA is rigorously tested on four engineering design optimization problems. Results demonstrated the robustness and superior performance of TNTWCOA in addressing complex engineering challenges.

Houssein et al. [28] presented a dynamic COA (DCOA) to tackle the challenge of premature convergence in the original COA. DCOA achieves this by generating dynamic opposite solutions at each iteration, effectively broadening the search space and preventing DCOA from getting trapped in local optima. This mechanism promotes diversity within the population and enhances the exploration of new regions and the exploitation of promising areas in the solution space. DCOA is further applied in a feature selection framework cooperating with the k-nearest neighbors (kNN) classifier. By identifying the most important attributes of input variables, DCOA refines the classification model and improves both accuracy and computational efficiency. Experimental results demonstrate that DCOA consistently outperforms other optimizers and showcases its superior ability to balance exploration and exploitation while achieving more robust and accurate classification performance.

Hashim et al. [29] proposed a modified COA (mCOA), where innovative operators are introduced to significantly boost its performance. First, an adaptive s-best mutation operator is integrated to dynamically balance exploration and exploitation by adjusting mutation rates based on solution quality. This operator enables mCOA to fine-tune the balance between diversifying the search space and intensifying the focus on promising regions. Second, a directional mutation rule is implemented, which strategically guides search efforts by steering mCOA toward the global best direction. This rule improves convergence speed and aids in navigating the solution landscape more effectively, which helps mCOA avoid local optima and enhance its global search capability. Benchmark tests in CEC2020 demonstrate the superiority of mCOA with improved accuracy and convergence compared to other algorithms. Furthermore, mCOA is applied for feature selection tasks. The experimental results reveal that the mCOA achieves the highest average performance on 75% of these datasets, which underscores its robustness and effectiveness in optimization challenges.

Hasanien et al. [30] introduced a novel enhanced COA (ECOA) with an efficient Lévy flight mechanism to update the population in each iteration. By integrating the Lévy flight distribution, ECOA injects greater diversity into the population and promotes broader exploration of the search space. Additionally, the Lévy flight enables the generation of new, high-potential solutions located in promising regions, which significantly reduces the probability of premature convergence and improves the capacity of ECOA to escape local optima. ECOA is specifically applied to complex optimization challenges within modern power systems, including the critical task of determining probabilistic optimal power flow (POPF). This application demonstrates the robust capability of ECOA in nonlinear search domains typical

of power systems and achieves reliable and accurate solutions for POPF. The experimental results underscore the effectiveness of ECOA in optimizing power flow under uncertainty.

Sundeep et al. [31] presented a novel COA-optimized Deep Convolutional Forest (COA-DCF) model, which integrates COA into the DFC classifier to enhance prediction accuracy. COA is employed to optimize the training process of the DCF, fine-tuning the parameters of the model and improving its ability to capture complex patterns in data. The proposed COA-DCF model is applied to predict ocean surface temperature anomalies, which is a critical issue in environmental and climate research. By incorporating key variables of sea surface temperature (SST), sea surface height (SSH), soil moisture, and wind speed, COA-DCF benefits the strengths of both the global searchability of COA and the robustness of the DCF classifier. Experimental results demonstrate that the proposed COA-DCF method significantly improves the overall performance of the deep learning model and provides more accurate and reliable predictions of ocean surface temperature anomalies, which can inform climate change studies and oceanographic forecasting.

Houssein et al. [32] presented an enhanced COA (eCOA) by integrating elements of the Runge–Kutta Optimizer (RUN) algorithm and resulting in a more powerful hybrid approach. eCOA leverages two core mechanisms from the RUN algorithm: the Scale Factor (SF) and Enhanced Solution Quality (ESQ). The SF mechanism enables fine-tuned control over step sizes of eCOA and improves the search precision, while the ESQ mechanism is integrated to refine solution quality iteratively and address the limitations of convergence and accuracy in the original COA. Simultaneously, these mechanisms significantly boost the algorithm's robustness and global optimization performance. The improved eCOA is applied to global optimization tasks and a practical feature selection problem in EEG data for emotion recognition. Experimental results confirm that eCOA excels in standard global optimization scenarios and holds substantial promise in advancing feature selection for complex, high-dimensional datasets like EEG, which highlights its utility in emotion recognition applications.

Miao et al. [33] introduced an efficient variant of COA named OCLCOA, which integrates a dynamic opposing learning search method to enhance the interaction among individuals within the population. By leveraging this approach, OCLCOA actively adjusts both the search direction and step size based on covariance matrix learning strategies. This adaptive adjustment enhances global searchability by guiding individuals toward promising regions of the solution space, thereby improving convergence rates and solution quality. Additionally, the covariance matrix approach fosters robustness in uncertain and dynamic environments by capturing the underlying patterns in population movements and adjusting search trajectories accordingly. The two integrated strategies effectively address two primary limitations in the original COA: limited interaction among population members and insufficient exploration capacity. Furthermore, OCLCOA is applied to the challenge of drone path planning in marine environments. Experimental results highlight the efficacy of OCLCOA and demonstrate its robust ability to identify efficient and reliable paths for drones navigating maritime environments, even in the face of environmental uncertainties and obstacles.

Although numerous improved variants of COA have been proposed, they still face persistent challenges such as an imbalance between exploration and exploitation, as well as premature convergence, particularly in complex and high-dimensional optimization problems. These limitations hinder the ability of COA to consistently achieve optimal solutions across diverse problem landscapes. To address these issues, integrating multiple search strategies and adaptive parameter control mechanisms has emerged as a promising direction, which provides the foundation and motivation for this research. Therefore, this paper introduces an enhanced variant termed MSICOA, which incorporates three innovative components: (1) a nonlinear inertia weight factor, (2) a Harris Hawk besieging mechanism, and (3) a spar-

row vigilant mechanism. These strategies synergistically improve the overall performance of MSICOA and enable it to effectively tackle complex optimization problems while mitigating issues of stagnation and premature convergence.

3 Our proposal: multi-strategies improved COA (MSICOA)

This section introduces our proposed MSICOA in detail. Figure 2 presents the flowchart of MSICOA, where the integrated components are highlighted in red.

At the beginning, the optimization problem is defined, the parameters of MSICOA are initialized, and the initial coati swarm is constructed and evaluated. Then, MSICOA enters the exploration phase and updates candidate individuals using the nonlinear inertia weight factor integrated hunting operator and the Harris Hawk besieging mechanism. The enhancements boost the searchability and adaptability of MSICOA. By integrating advanced strategies for movement and coordination, MSICOA effectively diversifies the search patterns and population diversity, which can avoid premature convergence.

Subsequently, MSICOA enters the exploitation phase and updates coati individuals using the sparrow vigilant mechanism. The vigilance mechanism incorporated into the MSICOA strengthens the alertness of MSICOA during the later stages of optimization, which simulates the natural vigilance and cautiousness observed in sparrows and enables the coatis to maintain a heightened sensitivity to their surroundings as they near potential solutions. The switch between the exploration phase and the exploitation phase in MSICOA is repeated until the computational resources are exhausted or the optimum is found. In the following context, we will detail the integrated three strategies.

3.1 Nonlinear inertia weighting factors

In the exploration of MSICOA, the process of updating the position of each coati in the tree is strongly influenced by its current location within the search space. This dependency is pivotal because it directly impacts the balance of MSICOA between intensification and diversification. To enhance this adaptability, a nonlinear inertia weight factor ω formulated is introduced, which modulates the relationship between the position of the current coati individual and its updated position during the search process. Equation (7) formulates the nonlinear inertia weighting factor integrated exploration strategy to replace Eq. (3). By adjusting this correlation, the nonlinear inertia weight factor enables MSICOA to emphasize global exploration and improve optimization accuracy while accelerating convergence.

$$\begin{aligned} \omega &= \frac{\mathrm{e}^{t/T} - 1}{\mathrm{e} - 1} \\ \boldsymbol{x}_{i,j}^{t+1} &= \omega \cdot \boldsymbol{x}_{i,j}^{t} + r \cdot \left(\boldsymbol{x}_{best,j} - I \cdot \boldsymbol{x}_{i,j}^{t} \right) \end{aligned} \tag{7}$$

Figure 3 presents the variation of ω as optimization progresses.

At the start of the MSICOA iteration, the inertia weight factor ω is set to a relatively low value. This relatively low initial value minimizes the influence of the current position of the coati on its movement updates and allows MSICOA to explore the search space comprehensively. By reducing positional dependency in this early phase, MSICOA gains an improved global exploration capability and allows to search for a broader range of potential

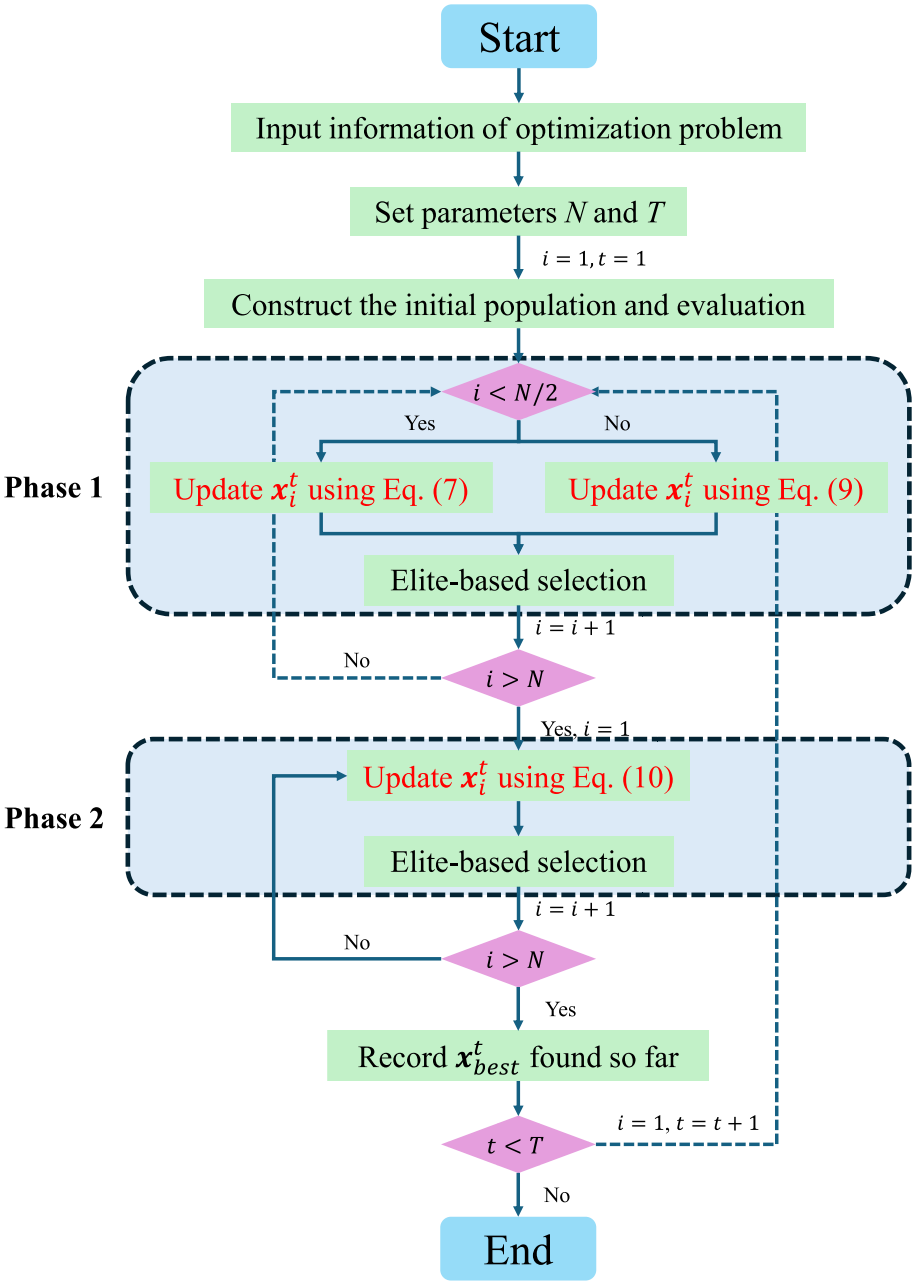

Fig. 2 The flowchart of MSICOA

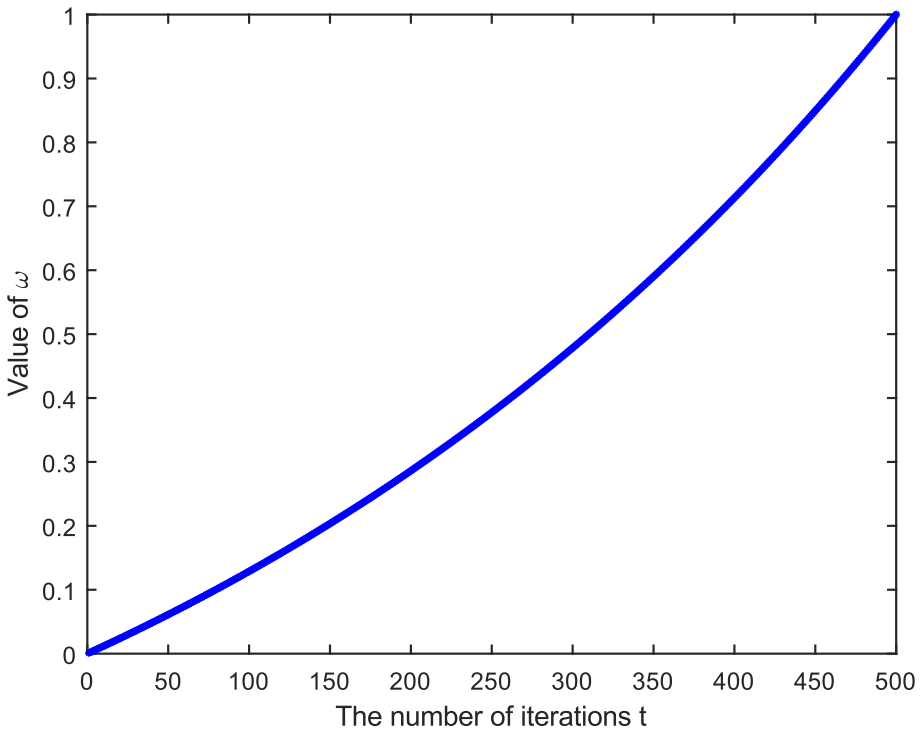

Fig. 3 Variation of ω with the number of iterations

solutions. This wide-ranging search contributes to MSICOA avoiding premature convergence and locating diverse, promising areas within the search landscape.

As the iteration progresses and the search gradually approaches optimal solutions, the value of ω increases incrementally. This gradual rise causes the position update of each coati to be more influenced by its current position and efficiently narrows the search domain. This shift fosters more focused, local exploration in areas of interest, enhancing the ability of MSICOA to refine potential solutions with greater precision. Consequently, the increase in ω enables MSICOA to concentrate on optimizing within high-quality solution regions, which accelerates convergence and improves accuracy in locating the optimal solution.

3.2 Harris Hawk besieging mechanism

In enhancing the position updating strategy for the under-tree coatis, the Harris Hawk siege mechanism from Harris Hawk Optimization (HHO) [34] is incorporated to improve their hunting efficiency and convergence capabilities. In this siege mechanism, Harris Hawks form a circular encirclement around their target and create a constrained zone to reduce the escape probability of prey. The Hawks maintain a tight formation, constantly adjusting their positions to increase pressure and capitalize on any opportunity to attack. However, the prey may attempt to escape and initiate an energy drain process during each evasion attempt, which is modeled by dynamically reducing the prey's energy level and mirrors the idea of gradually decreasing the search space. As iterations increase, the escape energy E of prey

gradually decreases, as defined in Eq. (8).

$$E = 2E_0(1 - t/T) \tag{8}$$

where E_0 in $(-1, 1)$ denotes the initial escape energy, and the integrated Harris Hawk besieging mechanism is formulated in Eq. (9).

$$\begin{aligned} \boldsymbol{x}_i^{t+1} &= \begin{cases} \boldsymbol{x}_{best}^t - E \cdot |J \cdot \boldsymbol{x}_{best}^t - \boldsymbol{x}_i^t|, & \text{if } r > 0.5 \\ \boldsymbol{x}_{best}^t - E \cdot |J \cdot \boldsymbol{x}_{best}^t - \boldsymbol{x}_i^t| + \text{Lévy}, & \text{otherwise} \end{cases} \\ J &= 2 \cdot (1 - r) \end{aligned} \tag{9}$$

This intelligent hunting strategy is applied to the second group of coatis that surround iguanas in MSICOA. Similar to the Harris Hawk, coatis encircle the iguana and launch a coordinated attack, with the iguana exhibiting a certain probability of escape. The escape energy of iguanas E decreases as the optimization progresses, which reduces its evasion capacity gradually. The incorporation of this siege mechanism enhances the efficiency of MSICOA in performing a global search across the space domain while maintaining effective local exploitation and ultimately improving the ability of MSICOA to tackle complex problems by balancing wide exploration with focused exploitation.

3.3 Sparrow vigilant mechanism

The vigilance mechanism in Sparrow Search Algorithm (SSA) [35] emulates the behavior of sparrows that maintain awareness of their surroundings during foraging. When a vigilant sparrow detects a predator or any perceived threat, it signals an early warning to the group and prompts the entire population to react by dispersing to evade the danger. This mechanism introduces a dynamic, adaptive layer to the SSA, as it allows the SSA to adjust the positions of individuals, maintaining diversity within the population and preventing premature convergence to local optima. Therefore, the motivation is to integrate this vigilance mechanism into MSICOA, as formulated in Eq. (10).

$$\boldsymbol{x}_i^{t+1} = \begin{cases} \boldsymbol{x}_{best}^t + \beta \cdot |\boldsymbol{x}_i^t - \boldsymbol{x}_{best}^t|, & \text{if } f(\boldsymbol{x}_i^t) > f(\boldsymbol{x}_{best}^t) \\ \boldsymbol{x}_i^t + K \cdot \left(\frac{|\boldsymbol{x}_i^t - \boldsymbol{x}_{worst}^t|}{f(\boldsymbol{x}_i^t) - f(\boldsymbol{x}_{worst}^t) + \varepsilon} \right), & \text{otherwise} \end{cases} \tag{10}$$

where β sampled from a standard normal distribution is a step control parameter, K in $(-1, 1)$ denotes the moving direction of coatis, and ε is a tiny number to avoid the zero division error. Replacing the escaping mechanism from Eq. (5) by Eq. (10), an adaptive and threat-aware movement strategy is introduced to strengthen the resilience of MSICOA against local optima entrapment. This approach significantly boosts MSICOA search efficiency and allows the search direction to adaptively focus on both diverse global search and precision-driven local refinement.

In summary, the pseudocode of the proposed MSICOA is presented in Algorithm 2.

3.4 Computational complexity of MSICOA

In MSICOA, initialization begins by setting the population size N and initializing the coati swarm in the search space. Since the dimension size of the problem is D, the time complexity for initialization is $O(N \cdot D)$. Subsequently, the exploration phase updates the positions of two groups of coatis independently, one group climbing trees and the other waiting in the

Algorithm 2 MSICOA

Require: Population size: N, Dimension: D, Maximum iteration: T
Ensure: Optimum: $\boldsymbol{x}_{best}$
Initialize coati swarm using Eq. (1)
$t = 1$
while $t \leq T$ **do**
  Divide coati swarm into two groups using Eq. (2)
  ► **Exploration Phase**
  The previous group of coatis updates using Eq. (7) # nonlinear inertia weighting factors
  The later group of coatis updates using Eq. (9) # Harris Hawk besieging mechanism
  Elite-based selection using Eq. (6)
  ► **Exploitation Phase**
  Coatis escape from predators using Eq. (10) # sparrow vigilant mechanism
  Elite-based selection using Eq. (6)
  Record $\boldsymbol{x}_{best}$
end while
return $\boldsymbol{x}_{best}$

ground. Each group performs position updates based on respective strategies and consumes $O(N \cdot D)$ computational budget in this phase.

In the exploitation phase, each coati adjusts its position using the sparrow vigilant mechanism. Since all coati individuals are involved, the time complexity for this stage also remains $O(N \cdot D)$. Given that the algorithm requires T iterations to converge, the total computational complexity of MSICOA is $O(T \cdot N \cdot D)$, which is consistent with the original COA theoretically. While the complexity between MSICOA and COA remains unchanged, the enhanced mechanisms introduce extra parameters and conditional identifications, which may marginally increase the actual runtime of MSICOA. However, this slight increase in runtime can be ignored by the improved search efficiency and convergence speed, which enables MSICOA to be a more effective variant of COA for complex optimization challenges.

4 Numerical experiments in CEC benchmarks

This section presents the numerical experiments in CEC benchmarks. Section 4.1 details the experimental settings including experimental environments and competitor algorithms. Section 4.2 summarizes the experimental results and statistical analysis.

4.1 Experimental settings

4.1.1 Experimental environments

To validate the effectiveness of the proposed improvement strategies and evaluate the feasibility and performance superiority of MSICOA compared to other optimizers, extensive simulation experiments are conducted in the CEC2017 [37] and CEC2020 [38] benchmarks, which are provided by the Opfunu library [39]. All simulations are executed in Python 3.11. The software and hardware environment used for the experiments included:

- Operating System: Windows 10 Professional 64-bit
- Processor: AMD A8-5600K APU with Radeon™ HD Graphics
- Clock Speed: 3.60 GHz
- Memory: 16 GB RAM

Table 1 The parameters of all compared optimization methods

Alg	Parameters and value
CS	N: 50; p_a: 0.25
WOA	N: 50; Constant b: 1
HGSO	N: 50; N_c: 5; M_1 and M_2: 0.1 and 0.2; α, β, K: 1
AVOA	N: 50; p_1, p_2, and p_3: 0.6, 0.4, and 0.6; α: 0.8; γ: 2.5
AGTO	N: 50; p_1 and p_2: 0.03 and 0.8; β: 3
GJO	N: 50
HBA	N: 50; β: 6; C: 2
EVO	N: 50
COA	N: 50
ICOA	N: 50; v: 0.3; α: [1,2)
CCOA	N: 50
MSICOA	N: 50

The maximum fitness evaluations of optimizers are fixed at 1000 · D (D = dimension size), respectively. To ensure statistical significance, each optimizer is repeated 20 times

This detailed setup ensures reliable performance during intensive computational tasks and reproducibility of this research.

4.1.2 Competitor algorithms and parameters

This section summarizes the competitor algorithms and their parameters. To ensure a fair and comprehensive evaluation, we select four categories of optimizers for comparison, which are listed as follows.

- Well-known optimizers: Cuckoo search (CS) [40], whale optimization algorithm (WOA) [41], and Henry gas solubility optimization (HGSO) [42].
- Recently proposed optimizers: African vulture optimization algorithm (AVOA) [43], artificial gorilla troops optimizer (AGTO) [12], golden jackal optimization (GJO) [44], honey badger algorithm (HBA) [45], energy valley optimizer (EVO) [46].
- COA and its variants: COA [23], improved COA (ICOA) [47], and cooperative COA (CCOA) [48].

These optimizers are partially provided by the Mealpy library [49]. Table 1 summarizes the detailed parameter settings.

4.2 Experimental results

This section presents the experimental results and statistical analysis. Section 4.2.1 demonstrates the results in CEC2017 and CEC2020, while the ablation experiments are presented in Sect. 4.2.2.

4.2.1 Comparison experiments in CEC benchmarks

This section presents the comparison experiments in CEC benchmarks. To identify the statistical significance between the proposed MSICOA and the competitor algorithms, the

Mann–Whitney U test is employed for every pairwise optimizer, while the Holm multiple comparison test is subsequently adopted to correct the p value obtained from the previous Mann–Whitney U test. Symbols of $+$, $\approx$, and $-$ denote that MSICOA is significantly better (i.e., the average fitness of MSICOA is better, and the p value is smaller than 0.05), without statistical significance (i.e., the p value is larger than 0.05), and significantly worse (i.e., the average fitness of MSICOA is worse, and the p value is smaller than 0.05) than the specific competitor algorithm. The Friedman test is employed to compute the average rank of optimizers and the best value is in bold. Furthermore, the quantitative analysis for the proportion between exploration and exploitation defined in [50] is employed, which is formulated in Eq. (11).

$$\begin{aligned} Div^t &= \frac{1}{D}\sum_{d=1}^{D}\frac{1}{N}\sum_{i=1}^{N}|\boldsymbol{x}^t_{\text{mean},d} - \boldsymbol{x}^t_{i,d}| \\ \text{Exploration} &= \frac{Div^t}{Div_{\max}} \\ \text{Exploitation} &= \frac{|Div^t - Div_{\max}|}{Div_{\max}} \end{aligned} \tag{11}$$

where $\boldsymbol{x}^t_{\text{mean}}$ is the centroid of the population. Table 2 summarizes the statistical significance and average ranks of optimizers in CEC benchmarks, while the detailed results are presented in "Appendices A and B". Furthermore, Figs. 4, 5, 6, and 7 present the convergence curves, boxplots, proportion between exploration and exploitation, and ranks of optimizers in CEC2017 (i.e., unimodal function f_1, multimodal functions f_4 and f_9, hybrid function f_{14}, and composite functions f_{22} and f_{30}) and CEC2020 (i.e., unimodal function f_1, multimodal functions f_2 and f_4, hybrid function f_6, and composite functions f_9 and f_{10}) representative functions.

The CEC2017 benchmark suite contains 29 functions while the CEC2020 suite includes 10 functions, which are carefully designed to evaluate optimizer performance on various optimization challenges. These functions are divided into unimodal, multimodal, hybrid, and composite types, each offering distinct complexities that investigate both local exploitation and global exploration capabilities of optimizers. Overall, our proposed MSICOA demonstrates strong competitive performance, ranking 2.2 and 2.0 in CEC2017 and 2.0 and 1.7 in CEC2020, respectively. These rankings highlight the robustness and effectiveness of MSICOA in tackling various optimization challenges. Specifically, in CEC2017, when compared to the second-best optimizer CCOA, MSICOA achieves a statistical summary of 15/9/5 and 14/9/6, while the comparison between MSICOA and the original COA is 29/0/0 and 29/0/0, which indicates a consistent edge across multiple test functions. Similarly, in CEC2020, MSICOA outperforms the competitors with a statistical summary of 3/5/2 against AGTO in the 10-D benchmark and 4/5/1 against AVOA. Moreover, MSICOA is significantly better than COA with statistical summaries of 10/0/0 and 10/0/0 on different scales, which further reinforces the capability of MSICOA to efficiently explore and exploit the search space.

In both CEC2017 and CEC2020, the first function, f_1, is an unimodal function featuring only a single optimum, which is capable of evaluating the exploitation and local searchability of algorithms. In this problem, MSICOA shows remarkable improvements, which effectively converge toward the optimum with higher precision compared to other COA variants and selected competitor algorithms. These results indicate that the integrated strategies in MSICOA significantly enhance its capability.

The remaining functions in CEC2017 and CEC2020 are multimodal, hybrid, and composite functions, each with multiple optima that present considerable challenges for optimizers.

Table 2 Statistical significance and average ranks of optimizers in CEC benchmarks

Bench	Dim	–	CS	WOA	HGSO	AVOA	AGTO	GJO	HBA	EVO	COA	ICOA	CCOA	MSICOA
CEC2017	50-D	+/≈/−	29/0/0	27/2/0	29/0/0	18/11/0	12/12/5	28/1/0	23/5/1	25/3/1	29/0/0	29/0/0	15/9/5	–
		Avg. rank	7.2	11.0	11.8	3.4	2.8	7.4	5.2	7.0	8.6	8.8	2.4	**2.2**
	100-D	+/≈/−	29/0/0	29/0/0	29/0/0	15/12/2	16/9/4	29/0/0	28/0/1	28/1/0	29/0/0	29/0/0	14/9/6	–
		Avg. rank	6.6	11.1	11.8	2.6	3.1	7.7	5.4	7.0	9.2	8.9	2.6	**2.0**
CEC2020	10-D	+/≈/−	10/0/0	9/1/0	10/0/0	6/4/0	3/5/2	10/0/0	8/2/0	10/0/0	10/0/0	10/0/0	8/2/0	–
		Avg. rank	7.3	11.0	12.0	4.0	2.1	7.1	4.3	8.7	8.3	7.9	3.3	**2.0**
	20-D	+/≈/−	10/0/0	9/1/0	10/0/0	4/5/1	9/0/1	10/0/0	8/2/0	10/0/0	10/0/0	10/0/0	8/2/0	–
		Avg. rank	6.6	11.1	11.8	2.7	3.2	7.6	4.1	8.4	8.9	8.5	3.4	**1.7**

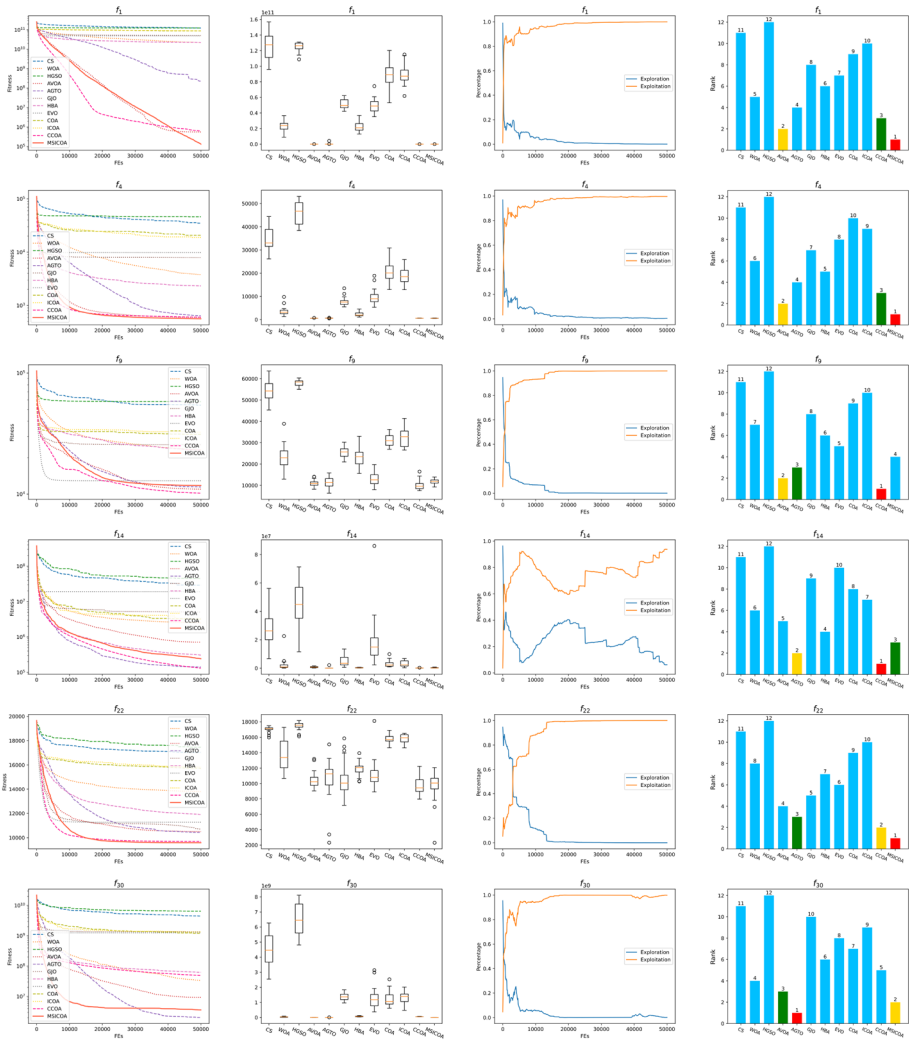

Fig. 4 Convergence curves, boxplots, proportion between exploration and exploitation, and ranks of optimizers in 50-D CEC2017 representative functions

These functions demand robust global searchability to identify various optimal regions and avoid local optima traps. Generally, MSICOA demonstrates exceptional performance, efficiently navigating through multiple peaks within the search domain. Statistical analysis and average rank comparisons further confirm the superiority of MSICOA, as it consistently outperforms other competitor algorithms in terms of accuracy, convergence speed, and robustness. These results affirm that the integration of the nonlinear inertia weight factor, Harris Hawk besieging mechanism, and sparrow vigilant mechanism can significantly strengthen the searchability of MSICOA on most functions.

Although the impressive performance of MSICOA has been observed, it demonstrates certain limitations when handling some multimodal functions, particularly when compared to CCOA, a variant that integrates cooperative mechanisms and optimal base vector strate-

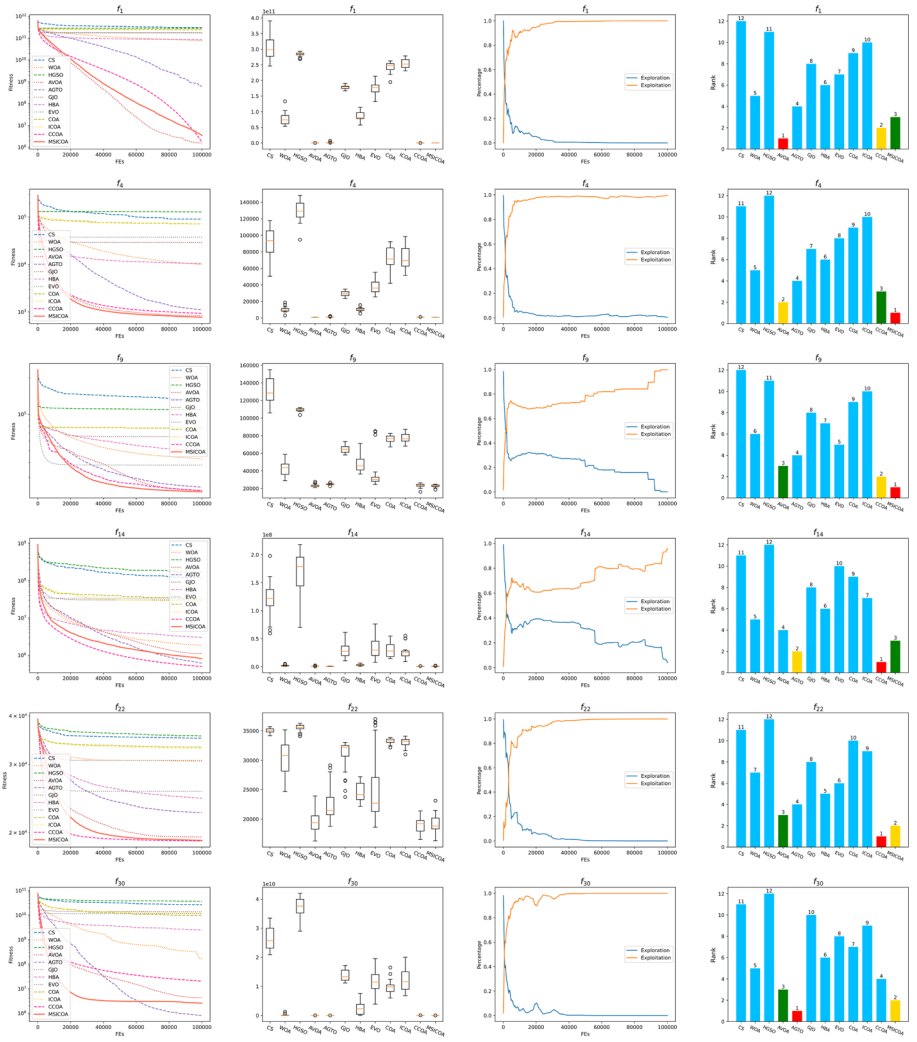

Fig. 5 Convergence curves, boxplots, proportion between exploration and exploitation, and ranks of optimizers in 100-D CEC2017 representative functions

gies. These enhancements enable CCOA to better tackle the complex landscapes typical of multimodal functions in the CEC2017 suite, as these strategies enhance collaboration among coati individuals and focus the search more effectively on promising regions. Nonetheless, compared to the original COA, MSICOA achieves statistically significant improvements across all test functions. The incorporated strategies collectively refine the balance of MSICOA between exploration and exploitation and increase its robustness against premature convergence. In summary, although CCOA may exhibit better performance in some multimodal scenarios, MSICOA represents a substantial advancement over the original COA. Its statistically significant improvements in various functions validate the success of MSICOA as an effective and versatile variant of COA.

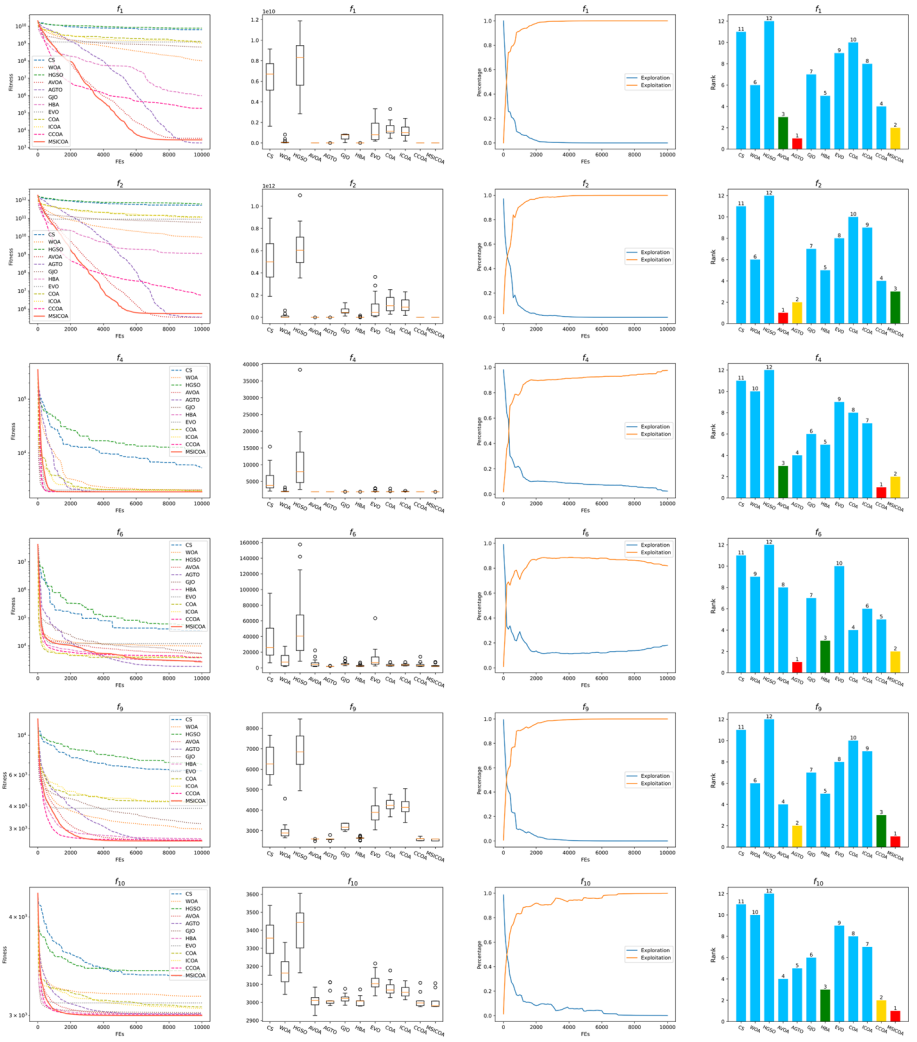

Fig. 6 Convergence curves, boxplots, proportion between exploration and exploitation, and ranks of optimizers in 10-D CEC2020 representative functions

4.2.2 Ablation experiments in CEC benchmarks

To identify the independent contribution of the integrated strategies of the nonlinear inertia weight factor, Harris Hawk besieging mechanism, and sparrow vigilant mechanism, this section presents the ablation experiments in CEC benchmarks. Here, COA is the baseline optimizer, COA-NIWF denotes COA + nonlinear inertia weight factor, COA-HHBM denotes COA + Harris Hawk besieging mechanism, COA-SVM denotes COA + sparrow vigilant mechanism, and MSICOA is the final proposal. Table 3 summarizes the statistical significance and average ranks of ablation experiments, while the detailed results are presented in "Appendix C".

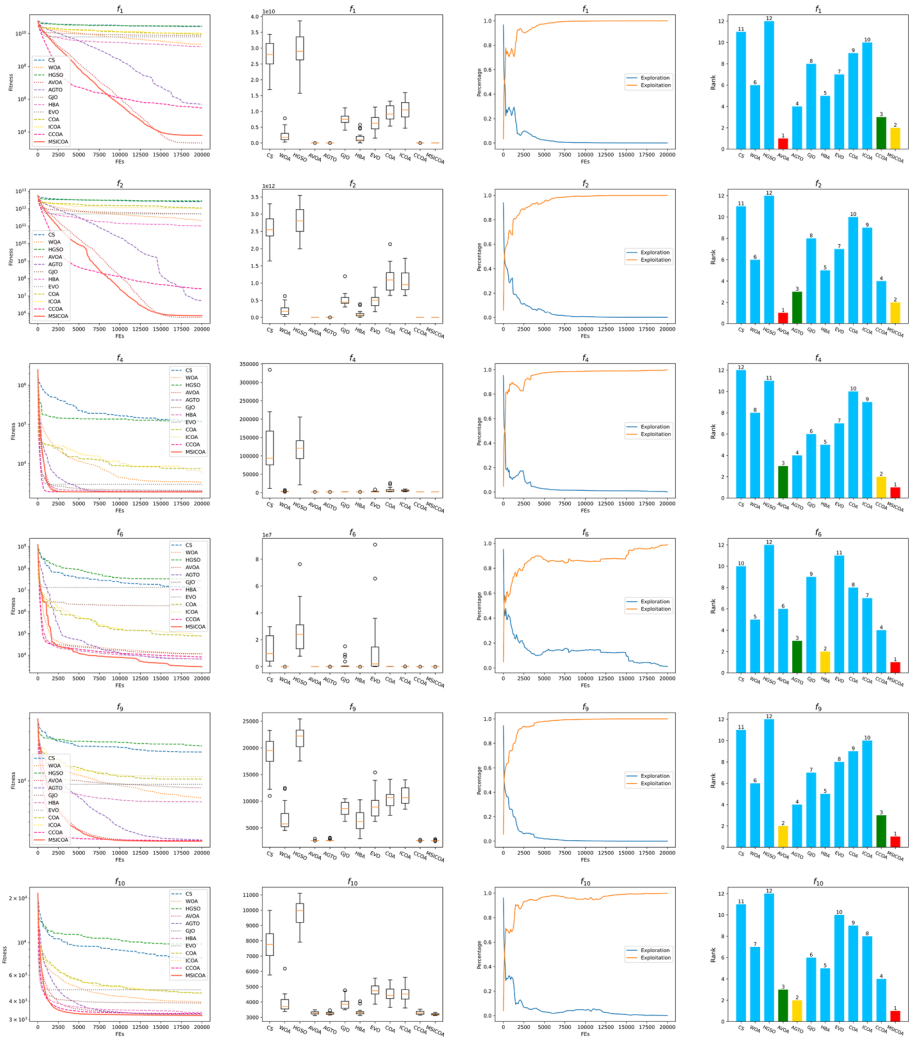

Fig. 7 Convergence curves, boxplots, proportion between exploration and exploitation, and ranks of optimizers in 20-D CEC2020 representative functions

The ablation study results reveal that each integrated strategy—nonlinear inertia weight factor, Harris Hawk besieging mechanism, and sparrow vigilant mechanism—contributes significantly to enhancing the performance of COA. Among these, the sparrow vigilant mechanism has the most substantial impact, offering notable improvements in diversity maintenance and local optima avoidance. This mechanism allows coatis to detect potential dangers and adjust their positions while reducing the risk of premature convergence.

Additionally, the contribution of other strategies cannot be neglected. The nonlinear inertia weight factor contributes to the adaptive exploration–exploitation balance and allows MSICOA to widen its search range initially and progressively refine its focus as it approaches optimal solutions, and the Harris Hawk besieging mechanism effectively strengthens the searchability by simulating coati attacks, which accelerates convergence around promising

Table 3 Statistical significance and average ranks of ablation experiments in CEC benchmarks

Bench	Dim	–	COA	COA-NIWF	COA-HHBM	COA-SVM	MSICOA
CEC2017	30-D	+/≈/−	–	1/1/27	0/1/28	0/2/27	0/0/29
		Avg. rank	4.9	3.2	2.7	**1.9**	2.2
	50-D	+/≈/−	–	1/0/28	0/1/28	0/0/29	0/0/29
		Avg. rank	4.9	3.2	2.6	2.3	**2.0**
CEC2020	10-D	+/≈/−	–	0/2/8	0/3/7	0/1/9	0/0/10
		Avg. rank	4.6	3.6	2.9	2.1	**1.8**
	20-D	+/≈/−	–	0/0/10	0/0/10	0/0/10	0/0/10
		Avg. rank	5.0	4.0	2.9	1.9	**1.2**

regions. Given these results, we recommend integrating all three strategies into COA to form MSICOA.

5 Application of MSICOA in engineering problems

This section applies our proposed MSICOA to handle classic engineering problems. Section 5.1 presents the problem definitions and parameters, while the detailed experimental results and analysis are summarized in Sect. 5.2.

5.1 Problem definitions and parameters

This section presents the problem definitions of involved engineering problems. Mathematical models of the Cantilever Beam Design Problem (CBDP), Corrugated Bulkhead Design Problem (CBHDP), Compression Spring Design Problem (CSDP), I-Beam Design Problem (IBDP), Three Bar Truss Design Problem (TBTDP), and Tubular Column Design Problem (TCDP) are as follows [51].

5.1.1 Cantilever beam design problem (CBDP)

CBDP is designed to withstand an applied load while ensuring that its deflection, stress, and natural frequency stay within acceptable limits. The design variables include the width and height of each segment of the beam, where the objective is to minimize the weight and volume of a cantilever beam. The mathematical model of CBDP is formulated in Eq. (12), and the demonstration is presented in Fig. 8.

$$\begin{aligned} &\textbf{min } f(X) = 0.0624(x_1 + x_2 + x_3 + x_4 + x_5) \\ &\textbf{s.t. } g(X) = \frac{61}{x_1^3} + \frac{37}{x_2^3} + \frac{19}{x_3^3} + \frac{7}{x_4^3} + \frac{1}{x_5^3} - 1 \leq 0 \\ &\textbf{where } 0.01 \leq x_i \leq 100,\ i \in \{1, 2, 3, 4, 5\} \end{aligned} \tag{12}$$

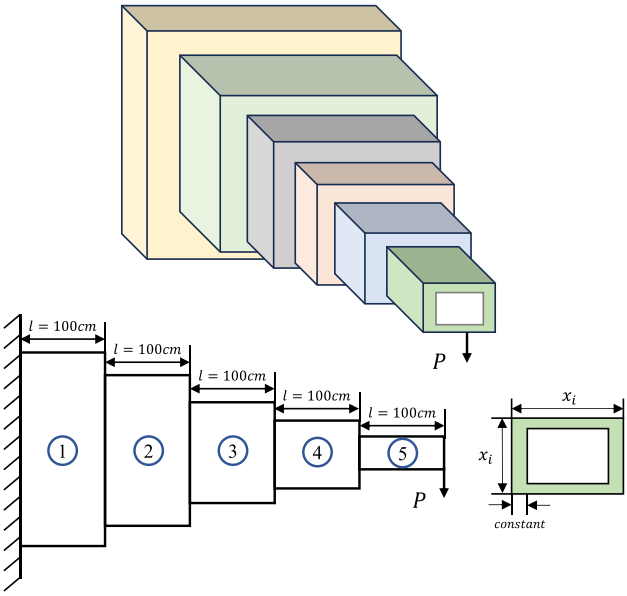

Fig. 8 A demonstration of CBDP

5.1.2 Corrugated bulkhead design problem (CBHDP)

CBHDP is an optimization problem in structural engineering that designing corrugated bulkheads to achieve maximum strength and rigidity with minimal weight. The mathematical model of CBHDP is formulated in Eq. (13).

$$
\begin{aligned}
\textbf{min}\ & f(X) = \frac{5.885x_4(x_1+x_3)}{x_1+\sqrt{|x_3^2-x_2^2|}} \\
\textbf{s.t.}\ & g_1(X) = -x_4x_2\left(0.4x_1+\frac{x_3}{6}\right)+8.94\left(x_1+\sqrt{|x_3^2-x_2^2|}\right) \le 0 \\
& g_2(X) = -x_4x_2^2\left(0.2x_1+\frac{x_3}{12}\right)+2.2\left(8.94\left(x_1+\sqrt{|x_3^2-x_2^2|}\right)\right)^{4/3} \le 0 \\
& g_3(X) = -x_4+0.0156x_1+0.15 \le 0 \\
& g_4(X) = -x_4+0.0156x_3+0.15 \le 0 \\
& g_5(X) = -x_4+1.05 \le 0 \\
& g_6(X) = -x_3+x_2 \le 0 \\
\textbf{where}\ & 0 \le x_1, x_2, x_3 \le 100 \\
& 0 \le x_4 \le 5
\end{aligned}
\tag{13}
$$

Fig. 9 A demonstration of CSDP

5.1.3 Compression spring design problem (CSDP)

CSDP is a classical engineering optimization that focuses on designing compression springs that meet specific load and deflection requirements while minimizing weight, cost, and size. The mathematical model of CSDP is formulated in Eq. (14), and the demonstration is presented in Fig. 9.

$$\begin{aligned}
\textbf{min}\ & f(X) = (x_3 + 2)x_2x_1^2 \\
\textbf{s.t.}\ & g_1(X) = 1 - \frac{x_2^3 x_3}{71785x_1^4} \leq 0 \\
& g_2(X) = \frac{4x_2^2 - x_1x_2}{12566(x_2x_1^3 - x_1^4)} \leq 0 \\
& g_3(X) = 1 - \frac{140.45x_1}{x_2^2x_3} \leq 0 \\
& g_4(X) = \frac{x_1 + x_2}{1.5} - 1 \leq 0 \\
\textbf{where}\ & 0.05 \leq x_1 \leq 2 \\
& 0.25 \leq x_2 \leq 1.3 \\
& 2 \leq x_3 \leq 15
\end{aligned} \tag{14}$$

5.1.4 I-beam design problem (IBDP)

IBDP is a structural optimization problem for designing an I-shaped beam to meet performance requirements while minimizing the material cost. The mathematical model of IBDP is formulated in Eq. (15), and the demonstration is presented in Fig. 10.

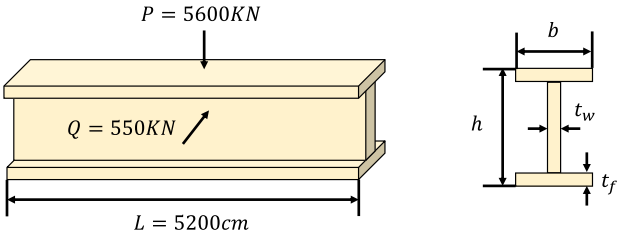

Fig. 10 A demonstration of IBDP

$$
\begin{aligned}
\textbf{min } f(X) &= \frac{500}{x_3(x_2-2x_4)^3/12 + (x_1x_4^3/6) + 2bx_4(x_2-x_4/2)^2} \\
\textbf{s.t. } g_1(X) &= 2x_1x_3 + x_3(x_2-2x_4) \le 300 \\
g_2(X) &= \frac{18x_2 \times 10^4}{x_3(x_2-2x_4)^3 + 2x_1x_3(4x_4^2 + 3x_2(x_2-2x_4))} \\
&\quad + \frac{15x_1 \times 10^3}{(x_2-2x_4)x_3^2 + 2x_3x_1^3} \le 56 \\
\textbf{where } & 10 \le x_1 \le 50 \\
& 10 \le x_2 \le 80 \\
& 0.9 \le x_3, x_4 \le 5
\end{aligned}
\tag{15}
$$

5.1.5 Three bar truss design problem (TBTDP)

TBTDP is a classic structural optimization problem that designing a simple truss structure to find an optimal set of cross-sectional areas for the bars in a three-bar truss while meeting load and displacement constraints. The mathematical model of TBTDP is formulated in Eq. (16), and the demonstration is presented in Fig. 11.

$$
\begin{aligned}
\textbf{min } f(X) &= \left(2\sqrt{2}x_1 + x_2\right) \cdot l \\
\textbf{s.t. } g_1(X) &= \frac{\sqrt{2}x_1 + x_2}{\sqrt{2}x_1^2 + 2x_1x_2} P - \sigma \le 0 \\
g_2(X) &= \frac{x_2}{\sqrt{2}x_1^2 + 2x_1x_2} P - \sigma \le 0 \\
g_3(X) &= \frac{1}{\sqrt{2}x_2 + x_1} P - \sigma \le 0 \\
& l = 100\,\text{cm},\ P = 2\,\text{kN/cm}^3,\ \sigma = 2\,\text{kN/cm}^3 \\
\textbf{where } & 0 \le x_1, x_2 \le 1
\end{aligned}
\tag{16}
$$

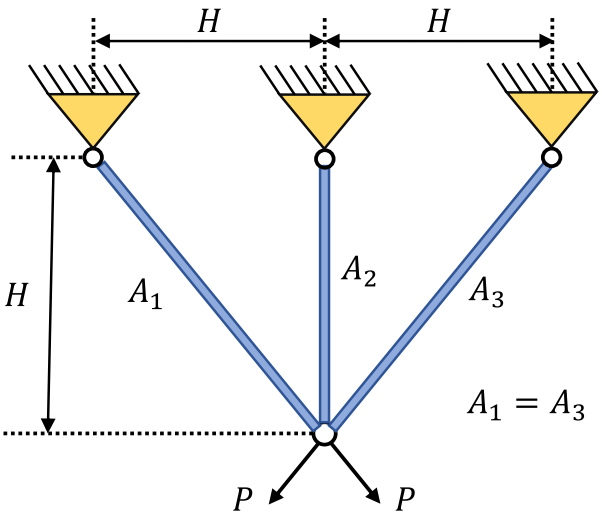

Fig. 11 A demonstration of TBTDP

5.1.6 Tubular column design problem (TCDP)

TCDP is an engineering optimization problem for designing a tubular column structure that meets load-bearing requirements while minimizing material usage, weight, and cost. The mathematical model of TCDP is formulated in Eq. (17), and the demonstration is presented in Fig. 12.

$$\begin{aligned} \textbf{min } & f(X) = 9.8x_1x_2 + 2x_1 \\ \textbf{s.t. } & g_1(X) = \frac{P}{\pi x_1 x_2 \sigma_y} - 1 \le 0 \\ & g_2(X) = \frac{8PL^2}{\pi^3 E x_1 x_2 (x_1^2 + x_2^2)} - 1 \le 0 \\ \textbf{where } & 2 \le x_1 \le 14 \\ & 0.2 \le x_2 \le 0.8 \end{aligned} \tag{17}$$

Population size and maximum fitness evaluations are fixed at 50 and 10,000, respectively, and the trial runs are 30. All engineering problems are provided by the Enoppy library [52]. Furthermore, we integrate static penalty function [53] into MSICOA and competitor algorithms and enable them to handle constrained engineering problems, which is defined in Eq. (18).

$$F(\boldsymbol{x}_i) = f(\boldsymbol{x}_i) + w \cdot \sum_{i=1}^{m} (\max(0, g_i(\boldsymbol{x}_i))) \tag{18}$$

where $F(\cdot)$ is the fitness function, $f(\cdot)$ is the objective function, $g_i(\cdot)$ is the constraint function, and $w = 10e7$ is a penalty constant.

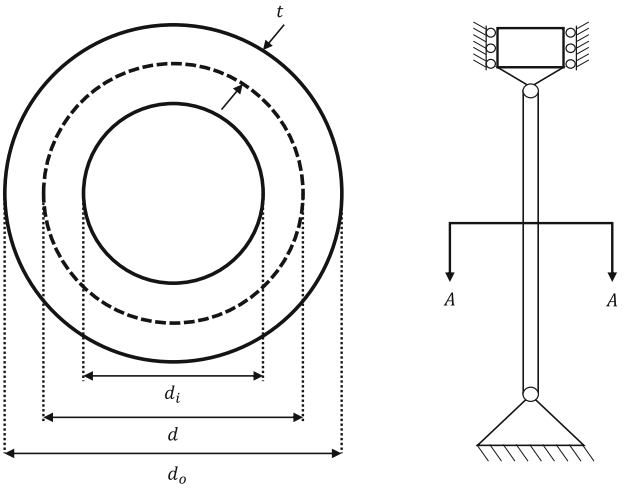

Fig. 12 A demonstration of TCDP

Table 4 Experimental results and statistical analysis in CBDP

Opt	Mean	Std	Best	Worst	*p* value
CS	4.188084e+00 +	6.073466e−01	2.730573e+00	5.361909e+00	6.796e−08
WOA	4.516790e+00 +	1.390762e+00	2.147921e+00	6.984207e+00	6.796e−08
HGSO	2.263098e+00 +	1.767516e−01	1.900056e+00	2.710069e+00	6.796e−08
AVOA	1.340676e+00 +	4.040057e−04	1.340076e+00	1.341383e+00	8.597e−06
AGTO	1.341549e+00 +	1.507551e−03	1.340090e+00	1.345578e+00	6.674e−06
GJO	1.340715e+00 +	5.025430e−04	1.340103e+00	1.341806e+00	5.874e−06
HBA	1.340953e+00 +	6.640953e−04	1.340059e+00	1.342617e+00	3.069e−06
EVO	2.669328e+00 +	7.238720e−01	1.861498e+00	4.911676e+00	6.796e−08
COA	1.671970e+00 +	1.760704e−01	1.386485e+00	2.181481e+00	6.796e−08
ICOA	1.678152e+00 +	2.500945e−01	1.361818e+00	2.338420e+00	6.796e−08
CCOA	1.417496e+00 +	9.624860e−02	1.345690e+00	1.785625e+00	6.796e−08
MSICOA	**1.340128e+00**	1.595733e−04	1.340011e+00	1.340542e+00	–

5.2 Experimental results and analysis

This section presents the detailed experimental results and statistical analysis of optimizers in engineering problems.

Experimental results in CBDP Table 4 presents the experimental results and statistical analysis of optimizers in CBDP, and Table 5 summarizes the information of optimal solutions obtained from optimizers, while convergence curves, boxplots, and ranks of optimizers are presented in Fig. 13.

Experimental results in CBHDP Table 6 presents the experimental results and statistical analysis of optimizers in CBHDP, and Table 7 summarizes the information of optimal solu-

Table 5 Optimal solutions obtained from optimizers in CBDP

Opt	x_1	x_2	x_3	x_4	x_5	$g(\boldsymbol{x})$	$f(\boldsymbol{x})$	$F(\boldsymbol{x})$
CS	7.39901488	17.87171872	5.42317284	7.4034429	5.66183107	− 0.70104155	2.730573e+00	2.730573e+00
WOA	5.18448212	4.19017876	12.82870839	5.28824504	6.93019506	0	2.147921e+00	2.147921e+00
HGSO	5.5072333	6.2274512	6.05574561	5.70661977	6.95257313	− 0.35539833	1.900056e+00	1.900056e+00
AVOA	6.01265783	5.30634371	4.47068803	3.55097537	2.13491643	− 2.96523051e−09	1.340076e+00	1.340076e+00
AGTO	5.99322191	5.286039	4.53952149	3.52714918	2.12986994	− 1.08341137e−06	1.340090e+00	1.340090e+00
GJO	6.0043843	5.27850021	4.53660502	3.49934048	2.15718228	− 0.00015998	1.340103e+00	1.340103e+00
HBA	5.98434618	5.28565947	4.52954699	3.51214858	2.16360385	− 5.30108663e−05	1.340059e+00	1.340059e+00
EVO	11.8067674	6.1510139	4.79290416	4.2402755	2.84074352	− 0.49594618	1.861498e+00	1.861498e+00
COA	6.54663921	4.43864192	5.08998254	3.52607372	2.61798138	− 2.31233824e−06	1.386485e+00	1.386485e+00
ICOA	5.75571422	5.21054622	4.28301388	4.36298938	2.21173962	− 3.4759205e−07	1.361818e+00	1.361818e+00
CCOA	5.74147904	5.72274401	4.42535195	3.56567559	2.11029838	− 0.00023176	1.345690e+00	1.345690e+00
MSICOA	6.05087899	5.31475428	4.47796673	3.49707656	2.13385935	− 8.27668156e−10	1.340011e+00	**1.340011e+00**

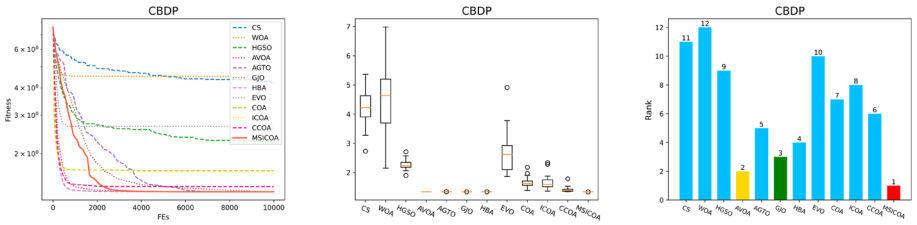

Fig. 13 Convergence curves, boxplots, and ranks of optimizers in CBDP

Table 6 Experimental results and statistical analysis in CBHDP

Opt	Mean	Std	Best	Worst	*p* value
CS	8.117933e+00 +	3.606858e−01	7.434773e+00	8.894608e+00	6.796e−08
WOA	7.918689e+00 +	1.115991e+00	6.865874e+00	1.202278e+01	6.796e−08
HGSO	9.905100e+00 +	1.137250e+00	8.125935e+00	1.198733e+01	6.796e−08
AVOA	8.882037e+00 +	1.778522e+00	6.947911e+00	1.451050e+01	6.796e−08
AGTO	6.845589e+00 +	6.716786e−03	6.842961e+00	6.872188e+00	6.557e−03
GJO	7.569714e+00 +	4.566559e−01	6.872824e+00	7.950135e+00	6.796e−08
HBA	6.848923e+00 +	6.613357e−03	6.843377e+00	6.866056e+00	2.563e−07
EVO	1.049911e+01 +	1.566409e+00	7.508090e+00	1.507679e+01	6.796e−08
COA	7.103841e+00 +	1.138797e−01	6.915754e+00	7.348650e+00	6.796e−08
ICOA	7.113607e+00 +	1.312345e−01	6.905706e+00	7.548128e+00	6.796e−08
CCOA	7.156473e+00 +	2.658532e−01	6.843869e+00	7.755141e+00	6.796e−08
MSICOA	**6.843145e+00**	4.729811e−04	6.842960e+00	6.845105e+00	–

tions obtained from optimizers, while convergence curves, boxplots, and ranks of optimizers are presented in Fig. 14.

Experimental results in CSDP Table 8 presents the experimental results and statistical analysis of optimizers in CSDP, and Table 9 summarizes the information of optimal solutions obtained from optimizers, while convergence curves, boxplots, and ranks of optimizers are presented in Fig. 15.

Experimental results in IBDP Table 10 presents the experimental results and statistical analysis of optimizers in IBDP, and Table 11 summarizes the information of optimal solutions obtained from optimizers, while convergence curves, boxplots, and ranks of optimizers are presented in Fig. 16.

Experimental results in TBTDP Table 12 presents the experimental results and statistical analysis of optimizers in TBTDP, and Table 13 summarizes the information of optimal solutions obtained from optimizers, while convergence curves, boxplots, and ranks of optimizers are presented in Fig. 17.

Experimental results in TCDP Table 14 presents the experimental results and statistical analysis of optimizers in TCDP, and Table 15 summarizes the information of optimal solutions obtained from optimizers, while convergence curves, boxplots, and ranks of optimizers are presented in Fig. 18.

Table 7 Optimal solutions obtained from optimizers in CBHDP

Opt	x_1	x_2	x_3	x_4	$g_1(\boldsymbol{x})$	$g_2(\boldsymbol{x})$	$g_3(\boldsymbol{x})$	$g_4(\boldsymbol{x})$	$g_5(\boldsymbol{x})$	$g_6(\boldsymbol{x})$	$f(\boldsymbol{x})$	$F(\boldsymbol{x})$
CS	54.89109147	36.9843028	50.77976981	1.07224703	−8.54506810e+02	−5.92027220e+03	−6.59459983e−02	−1.30082616e−01	−2.22470253e−02	−1.37954670e+01	7.434773e+00	7.434773e+00
WOA	57.69230763	34.55472734	57.56060262	1.05	−1.04723223e+03	−5.85620393e+02	−1.03471556e−09	−2.05459907e−03	−1.01252340e−13	−2.30058753e+01	6.865874e+00	6.865874e+00
HGSO	41.78673594	31.93461292	56.0044924	1.22156039	−9.97191698e+02	−2.97443034e+02	−4.19687310e−01	−1.97890309e−01	−1.71560391e−01	−2.40698795e+01	8.007476e+00	8.007476e+00
AVOA	52.65934486	34.1543703	55.73378363	1.05327164	−9.17275346e+02	−5.28284709e+02	−8.17858636e−02	−3.38246188e−02	−3.27164344e−03	−2.15794133e+01	6.947911e+00	6.947911e+00
AGTO	57.69229461	34.14759156	57.6921288	1.05000005	−1.04890504e+03	−5.09981623e−04	−2.53355272e−07	−2.83997659e−06	−4.92562424e−08	−2.35445372e+01	6.842961e+00	6.842961e+00
GJO	56.6676471	33.93422552	56.33987739	1.05039478	−9.88431830e+02	−2.47249854e+01	−1.63794877e−02	−2.14926953e−02	−3.94782488e−04	−2.24056519e+01	6.872824e+00	6.872824e+00
HBA	57.65339827	34.15017926	57.69282797	1.05000908	−1.04836760e+03	−3.97684327e+00	−6.16068990e−04	−9.65653580e−07	−9.08205413e−06	−2.35426487e+01	6.843377e+00	6.843377e+00
EVO	48.05078606	32.20321413	46.70281463	1.10240413	−6.58350841e+02	−9.23597052e+02	−2.02811865e−01	−2.23840219e−01	−5.24041275e−02	−1.44996005e+01	7.508090e+00	7.508090e+00
COA	52.65365558	34.19636957	56.23671771	1.05005123	−9.27335979e+02	−4.17813252e+02	−7.86541994e−02	−2.27584302e−02	−5.12265146e−05	−2.20403481e+01	6.915754e+00	6.915754e+00
ICOA	55.34840981	34.62530858	56.73809637	1.05000789	−9.85681205e+02	−8.65595792e+02	−3.65727005e−02	−1.48935902e−02	−7.89354359e−06	−2.21127878e+01	6.905706e+00	6.905706e+00
CCOA	57.68203346	34.15958535	57.69218336	1.05004077	−1.04890552e+03	−1.71964810e+01	−2.01052146e−04	−4.27137940e−05	−4.07741330e−05	−2.35325980e+01	6.843869e+00	6.843869e+00
MSICOA	57.69230592	34.14759189	57.6921287	1.05000001	−1.04890513e+03	−1.11040801e−04	−3.76480000e−08	−2.80228000e−06	−9.99999994e−09	−2.35445368e+01	6.842960e+00	6.842960e+00

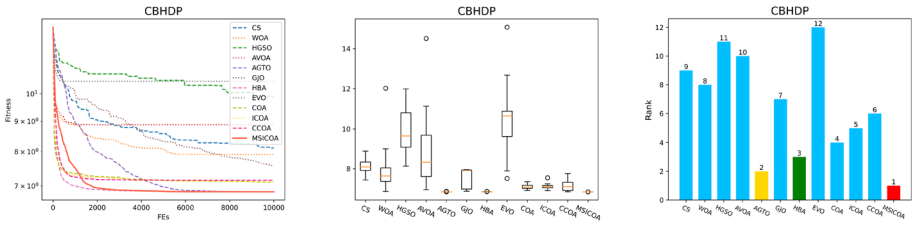

Fig. 14 Convergence curves, boxplots, and ranks of optimizers in CBHDP

Table 8 Experimental results and statistical analysis in CSDP

Opt	Mean	Std	Best	Worst	*p* value
CS	1.090223e−02 +	2.834808e−03	7.281849e−03	2.043712e−02	1.945e−08
WOA	6.568291e−03 +	8.837206e−04	6.076142e−03	9.703666e−03	1.973e−04
HGSO	1.313397e−02 +	4.035326e−03	7.699835e−03	2.434101e−02	1.945e−08
AVOA	6.076169e−03 +	9.113522e−08	6.076142e−03	6.076562e−03	1.945e−08
AGTO	**6.076142e−03** ≈	3.745823e−13	6.076142e−03	6.076142e−03	8.036e−02
GJO	6.077847e−03 +	1.070819e−06	6.076183e−03	6.080372e−03	1.945e−08
HBA	6.076142e−03 ≈	6.4246713e−14	6.076142e−03	6.076142e−03	8.036e−02
EVO	7.017373e−03 +	9.806777e−04	6.080706e−03	9.832370e−03	1.945e−08
COA	6.076153e−03 +	1.549315e−08	6.076142e−03	6.076191e−03	1.945e−08
ICOA	6.076150e−03 +	9.571921e−09	6.076142e−03	6.076175e−03	1.945e−08
CCOA	6.077928e−03 +	2.293346e−06	6.076171e−03	6.085065e−03	1.945e−08
MSICOA	**6.076142e−03**	2.602085e−18	6.076142e−03	6.076142e−03	–

The proposed MSICOA consistently achieves top ranks in solving six engineering design problems, which secures the 1st rank in five instances and the 2nd once. Specifically, MSICOA ranks 1st in CBDP, CBHDP, CSDP, IBDP, and TCDP, 2nd in TBTDP. These results underscore the highly competitive and versatile performance of MSICOA across different engineering challenges. Furthermore, the performance of MSICOA is either statistically equivalent to or significantly outperforms all optimizers across all problem instances. This performance is primarily attributed to integrated strategies in MSICOA—the nonlinear inertia weight factor, Harris Hawk besieging mechanism, and sparrow vigilance mechanism—which collectively enhance exploration, exploitation, and population diversity. The effectiveness of these strategies ensures a balanced search process and allows MSICOA to effectively navigate complex landscapes.

6 Conclusion

This paper presents the Multi-Strategies Improved Coati Optimization Algorithm (MSICOA), which integrates multiple enhancement strategies to boost search efficiency and solution quality compared with the original COA. A nonlinear inertia weight factor dynamically adjusts the influence of coatis' positions to ensure an adaptive balance between global exploration and local exploitation as optimization progresses, the Harris Hawk besieging mechanism introduces an effective prey-attack strategy that accelerates convergence toward high-potential

Table 9 Optimal solutions obtained from optimizers in CSDP

Opt	x_1	x_2	x_3	$g_1(\boldsymbol{x})$	$g_2(\boldsymbol{x})$	$g_3(\boldsymbol{x})$	$g_4(\boldsymbol{x})$	$f(\boldsymbol{x})$	$F(\boldsymbol{x})$
CS	0.05050318	0.69601476	2.10190598	−0.51760894	−0.35026064	−5.96610986	−0.50232137	7.281849e−03	7.281849e−03
WOA	0.05	0.60761419	2	−2.22044605e−16	−4.49469126e−01	−8.51055660e+00	−5.61590539e−01	6.076142e−03	6.076142e−03
HGSO	0.05	0.76998355	2	−1.03498218	−0.16001075	−4.92241534	−0.4533443	7.699835e−03	7.699835e−03
AVOA	0.05	0.60761419	2	−1.16773258e−12	−4.49469126e−01	−8.51055660e+00	−5.61590539e−01	6.076142e−03	6.076142e−03
AGTO	0.05	0.60761419	2	−2.22044605e−16	−4.49469126e−01	−8.51055660e+00	−5.61590539e−01	6.076142e−03	6.076142e−03
GJO	0.05	0.6076183	2	−2.03022576e−05	−4.49462668e−01	−8.51042788e+00	−5.61587798e−01	6.076183e−03	6.076183e−03
HBA	0.05	0.60761419	2	−2.22044605e−16	−4.49469126e−01	−8.51055660e+00	−5.61590539e−01	6.076142e−03	6.076142e−03
EVO	0.05	0.6080706	2	−2.25511403e−03	−4.48751993e−01	−8.49628516e+00	−5.61286270e−01	6.080706e−03	6.080706e−03
COA	0.05	0.60761419	2	−3.26827454e−12	-4.49469126e−01	−8.51055660e+00	−5.61590539e−01	6.076142e−03	6.076142e−03
ICOA	0.05	0.60761419	2	−3.58157948e−13	−4.49469126e−01	−8.51055660e+00	−5.61590539e−01	6.076142e−03	6.076142e−03
CCOA	0.05	0.60761711	2	−1.44001185e−05	−4.49464545e−01	−8.51046530e+00	−5.61588595e−01	6.076171e−03	6.076171e−03
MSICOA	0.05	0.60761419	2	−2.29816166e−12	−4.49469126e−01	−8.51055660e+00	−5.61590539e−01	6.076142e−03	6.076142e−03

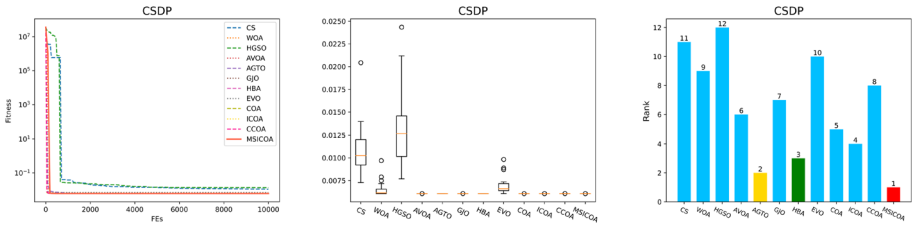

Fig. 15 Convergence curves, boxplots, and ranks of optimizers in CSDP

Table 10 Experimental results and statistical analysis in IBDP

Opt	Mean	Std	best	worst	*p* value
CS	2.106500e−04 +	1.934583e−05	1.761018e−04	2.548064e−04	1.942e−08
WOA	2.490157e−04 +	1.175305e−04	1.745821e−04	6.792201e−04	4.281e−05
HGSO	2.163395e−04 +	2.110628e−05	1.749168e−04	2.464404e−04	1.945e−08
AVOA	**1.745821e−04** +	2.053772e−14	1.745821e−04	1.745821e−04	1.945e−08
AGTO	**1.745821e−04** ≈	9.623731e−15	1.745821e−04	1.745821e−04	8.036e−02
GJO	1.745830e−04 +	7.371821e−10	1.745821e−04	1.745845e−04	1.945e−08
HBA	**1.745821e−04** +	2.413839e−16	1.745821e−04	1.745821e−04	1.945e−08
EVO	2.330700e−04 +	3.925969e−05	1.746729e−04	3.216734e−04	1.945e−08
COA	**1.745821e−04** +	1.163978e−11	1.745821e−04	1.745821e−04	1.945e−08
ICOA	**1.745821e−04** +	9.611630e−12	1.745821e−04	1.745821e−04	1.945e−08
CCOA	3.065216e−04 +	6.117163e−05	1.745821e−04	4.408716e−04	1.945e−08
MSICOA	**1.745821e−04**	8.131516e−20	1.745821e−04	1.745821e−04	–

Table 11 Optimal solutions obtained from optimizers in IBDP

Opt	x_1	x_2	x_3	x_4	$g_1(\boldsymbol{x})$	$g_2(\boldsymbol{x})$	$f(\boldsymbol{x})$	$F(\boldsymbol{x})$
CS	50	80	0.9	5	−147	−44.79736381	1.761018e−04	1.761018e−04
WOA	50	80	1.76470588	5	−6.25277607e−13	−5.02870668e+01	1.745821e−04	1.745821e−04
HGSO	50	80	1.57301806	5	−32.58693064	−49.59078709	1.749167e−04	1.749167e−04
AVOA	50	80	1.76470588	5	−9.37916411e−11	−5.02870668e+01	1.745821e−04	1.745821e−04
AGTO	50	80	1.76470588	5	−5.68434189e−14	−5.02870668e+01	1.745821e−04	1.745821e−04
GJO	50	80	1.76465048	5	−9.41798763e−03	−5.02868875e+01	1.745821e−04	1.745821e−04
HBA	50	80	1.76470588	5	−3.35376171e−12	−5.02870668e+01	1.745821e−04	1.745821e−04
EVO	50	80	1.71260201	5	−8.85765805	−50.11323214	1.746729e−04	1.746729e−04
COA	50	80	1.76470578	5	−1.73244575e−05	−5.02870665e+01	1.745821e−04	1.745821e−04
ICOA	50	80	1.76470574	5	−2.50469200e−05	−5.02870664e+01	1.745821e−04	1.745821e−04
CCOA	50	80	1.76469067	5	−2.58686649e−03	−5.02870176e+01	1.745821e−04	1.745821e−04
MSICOA	50	80	1.76470588	5	−9.11200004e−11	−5.02870668e+01	1.745821e−04	1.745821e−04

regions, and the sparrow vigilance mechanism enhances the alertness and adaptability of the coati swarm, guiding individuals toward safer and more optimal search zones. These synergistic modifications collectively enhance the precision, robustness, and efficiency of MSICOA.

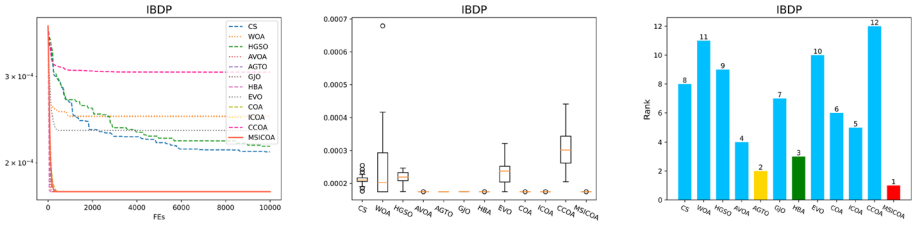

Fig. 16 Convergence curves, boxplots, and ranks of optimizers in IBDP

Table 12 Experimental results and statistical analysis in TBTDP

Opt	Mean	Std	Best	Worst	*p* value
CS	2.647549e+02 +	5.669353e−01	2.640731e+02	2.663835e+02	6.796e−08
WOA	2.669419e+02 +	3.277157e+00	2.639125e+02	2.767005e+02	7.898e−08
HGSO	2.652913e+02 +	1.005381e+00	2.641587e+02	2.677557e+02	6.796e−08
AVOA	2.639154e+02 +	3.425353e−02	2.638958e+02	2.640370e+02	1.436e−02
AGTO	2.638996e+02 ≈	7.019913e−03	2.638958e+02	2.639222e+02	1.199e−01
GJO	2.698657e+02 +	3.716974e+00	2.649146e+02	2.761453e+02	6.796e−08
HBA	2.639030e+02 ≈	1.006420e−02	2.638958e+02	2.639298e+02	3.942e−01
EVO	2.670484e+02 +	3.563000e+00	2.642991e+02	2.769502e+02	6.796e−08
COA	2.639021e+02 ≈	9.358675e−03	2.638960e+02	2.639384e+02	2.503e−01
ICOA	**2.638988e+02** ≈	2.876078e−03	2.638960e+02	2.639059e+02	5.979e−01
CCOA	2.645373e+02 +	1.286376e+00	2.638987e+02	2.696096e+02	1.600e−05
MSICOA	2.638993e+02	5.709528e−03	2.638960e+02	2.639220e+02	–

Through rigorous numerical experiments in CEC2017 and CEC2020, the effectiveness of MSICOA has been thoroughly validated. Comparative analysis against state-of-the-art optimizers and advanced COA variants demonstrates that MSICOA excels in convergence accuracy and solution stability. Additionally, MSICOA has exhibited superior performance in real-world engineering simulations, which further underscores the practicality and reliability of MSICOA for complex engineering applications.

Nevertheless, it is important to acknowledge the current application scope of MSICOA. While the proposed algorithm has demonstrated remarkable optimization capabilities, its potential extends beyond the tested domains. Future research will focus on expanding its applicability to intelligent transportation systems, energy management, bioinformatics, and other interdisciplinary fields. We believe that MSICOA has the potential to serve as a powerful and adaptable optimization tool across diverse real-world scenarios.

Table 13 Optimal solutions obtained from optimizers in TBTDP

Opt	x_1	x_2	$g_1(\boldsymbol{x})$	$g_2(\boldsymbol{x})$	$g_3(\boldsymbol{x})$	$f(\boldsymbol{x})$	$F(\boldsymbol{x})$
CS	0.79165878	0.40158133	− 0.00130855	− 1.28521002	− 0.52895806	2.640731e+02	2.640731e+02
WOA	0.79347365	0.39484247	0	− 1.29542799	− 0.52056258	2.639125e+02	2.639125e+02
HGSO	0.80674257	0.35977428	− 3.03224493e−04	− 1.35155383e+00	− 4.79712019e−01	2.641587e+02	2.641587e+02
AVOA	0.78864804	0.40832493	− 2.33483233e−10	− 1.27420085e+00	− 5.35985502e−01	2.638958e+02	2.638958e+02
AGTO	0.78867674	0.40824376	0	− 1.27432812	− 0.53589323	2.638958e+02	2.638958e+02
GJO	0.77259136	0.46392745	− 0.00570978	− 1.19048727	− 0.60011016	2.649146e+02	2.649146e+02
HBA	0.78871973	0.40812216	− 9.68336522e−13	− 1.27451879e+00	− 5.35754994e−01	2.638958e+02	2.638958e+02
EVO	0.78904881	0.41122416	− 0.00304784	− 1.27064004	− 0.54079314	2.642991e+02	2.642991e+02
COA	0.78829217	0.40933275	− 1.43977495e−07	− 1.27262117e+00	− 5.37130649e−01	2.638960e+02	2.638960e+02
ICOA	0.78904316	0.40720908	− 5.57823082e−07	− 1.27595123e+00	− 5.34716694e−01	2.638960e+02	2.638960e+02
CCOA	0.78867491	0.4082773	− 2.14981493e−05	− 1.27428241e+00	− 5.35942109e−01	2.638987e+02	2.638987e+02
MSICOA	0.78826251	0.40941663	− 2.03070893e−11	− 1.27248968e+00	− 5.37225833e−01	2.638960e+02	2.638960e+02

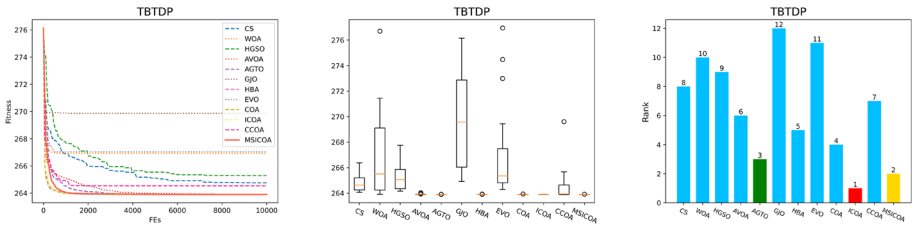

Fig. 17 Convergence curves, boxplots, and ranks of optimizers in TBTDP

Table 14 Experimental results and statistical analysis in TCDP

Opt	Mean	Std	best	worst	p value
CS	3.067101e+01 +	2.688446e−01	3.018544e+01	3.113722e+01	6.796e−08
WOA	3.176520e+01 +	1.225485e+00	3.028336e+01	3.606342e+01	6.467e−08
HGSO	3.084923e+01 +	3.586737e−01	3.028400e+01	3.155621e+01	6.796e−08
AVOA	3.015003e+01 +	5.710466e−04	3.014974e+01	3.015166e+01	7.898e−08
AGTO	**3.014974e+01** ≈	2.808195e−07	3.014974e+01	3.014974e+01	2.085e−01
GJO	3.017942e+01 +	2.575417e−02	3.015162e+01	3.025760e+01	6.796e−08
HBA	**3.014974e+01** ≈	1.367213e−08	3.014974e+01	3.014974e+01	1.806e−01
EVO	3.211864e+01 +	1.265867e+00	3.038133e+01	3.475135e+01	6.796e−08
COA	3.018478e+01 +	3.719950e−02	3.015020e+01	3.031263e+01	6.796e−08
ICOA	3.016415e+01 +	1.726916e−02	3.015088e+01	3.021606e+01	6.796e−08
CCOA	3.106364e+01 +	8.919787e−01	3.016423e+01	3.307415e+01	6.796e−08
MSICOA	**3.014974e+01**	1.089764e−08	3.014974e+01	3.014974e+01	–

Table 15 Optimal solutions obtained from optimizers in TCDP

Opt	x_1	x_2	$g_1(\boldsymbol{x})$	$g_2(\boldsymbol{x})$	$f(\boldsymbol{x})$	$F(\boldsymbol{x})$
CS	7.10507193	0.22943214	−0.00197203	−0.00256398	3.018544e+01	3.018544e+01
WOA	7.04996264	0.23423821	−0.01480797	0	3.028336e+01	3.028336e+01
HGSO	7.06328271	0.23342093	−0.01322289	−0.00215345	3.028400e+01	3.028400e+01
AVOA	7.10297475	0.2290473	−3.58509189e−09	−6.40312248e−11	3.014974e+01	3.014974e+01
AGTO	7.10297476	0.2290473	−2.55351296e−15	−7.02771175e−14	3.014974e+01	3.014974e+01
GJO	7.1026855	0.22909199	−1.54364035e−04	−7.34154312e−05	3.015162e+01	3.015162e+01
HBA	7.10297476	0.2290473	−5.55111512e−16	−2.08721929e−13	3.014974e+01	3.014974e+01
EVO	7.10878659	0.23201753	−0.01360882	−0.01524601	3.038133e+01	3.038133e+01
COA	7.10280608	0.22906417	−4.99186819e−05	−2.62766945e−06	3.015020e+01	3.015020e+01
ICOA	7.10339979	0.22903782	−1.84317280e−05	−1.37886117e−04	3.015088e+01	3.015088e+01
CCOA	7.10567997	0.22909057	−5.69527852e−04	−1.32997289e−03	3.016423e+01	3.016423e+01
MSICOA	7.10297479	0.2290473	−1.29223299e−11	−8.54671944e−09	3.014974e+01	3.014974e+01

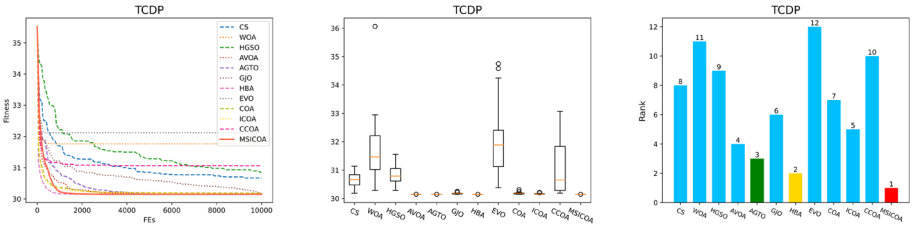

Fig. 18 Convergence curves, boxplots, and ranks of optimizers in TCDP

A: Experimental results in CEC2017

Tables 16 and 17 summarize the detailed experimental results in CEC2017, while the p values between MSICOA and competitor algorithms are summarized in Tables 18 and 19.

Table 16 Experimental results in 50-D CEC2017

Func.		CS	WOA	HGSO	AVOA	AGTO	GJO	HBA	EVO	COA	ICOA	CCOA	MSICOA
f_1	mean	1.245e+11 +	2.238e+10 +	1.249e+11 +	5.573e+05 +	2.286e+08 +	5.149e+10 +	2.245e+10 +	4.934e+10 +	8.835e+10 +	8.902e+10 +	6.268e+05 +	**1.327e+05**
	std	1.294e+06	9.117e+08	1.684e+10	6.607e+09	5.900e+09	6.105e+09	7.073e+09	9.205e+09	1.492e+10	1.202e+10	1.217e+05	9.571e+04
f_3	mean	2.879e+05 +	1.314e+05 +	3.681e+05 +	1.266e+05 +	**4.777e+04** −	1.783e+05 +	7.643e+04 −	6.187e+05 +	2.097e+05 +	2.087e+05 +	1.058e+05 +	9.971e+04
	std	1.564e+04	1.185e+04	3.223e+04	2.103e+04	5.093e+04	1.625e+04	1.338e+04	1.039e+06	3.114e+04	4.006e+04	1.729e+04	2.633e+04
f_4	mean	3.502e+04 +	3.807e+03 +	4.604e+04 +	5.976e+02 +	6.375e+02 +	7.888e+03 +	2.331e+03 +	9.834e+03 +	2.082e+04 +	1.894e+04 +	6.029e+02 +	**5.629e+02**
	std	5.865e+01	7.497e+01	5.219e+03	1.999e+03	4.915e+03	1.864e+03	9.646e+02	3.432e+03	5.009e+03	3.482e+03	3.437e+01	5.786e+01
f_5	mean	1.319e+03 +	1.068e+03 +	1.316e+03 +	8.570e+02 ≈	8.351e+02 ≈	1.065e+03 +	8.944e+02 +	8.658e+02 ≈	1.157e+03 +	1.153e+03 +	**7.761e+02** −	8.537e+02
	std	4.274e+01	5.322e+01	4.659e+01	1.290e+02	1.283e+01	1.956e+01	4.722e+01	3.083e+01	4.138e+01	3.264e+01	3.990e+01	3.276e+01
f_6	mean	7.103e+02 +	6.814e+02 +	7.225e+02 +	6.543e+02 ≈	6.577e+02 +	6.792e+02 +	6.630e+02 +	**6.443e+02** −	6.899e+02 +	6.912e+02 +	6.498e+02 ≈	6.518e+02
	std	6.275e+00	8.498e+00	6.498e+00	7.457e+00	4.447e+00	3.101e+00	3.322e+00	6.740e+00	5.116e+00	6.692e+00	3.885e+00	6.059e+00
f_7	mean	3.134e+03 +	1.824e+03 +	2.202e+03 +	1.491e+03 ≈	1.469e+03 ≈	1.561e+03 +	1.617e+03 +	1.639e+03 +	2.014e+03 +	2.017e+03 +	**1.150e+03** +	1.428e+03
	std	1.048e+02	1.396e+02	3.684e+02	1.490e+02	2.376e+01	7.494e+01	8.649e+01	9.483e+01	8.664e+01	5.885e+01	8.683e+01	1.297e+02
f_8	mean	1.632e+03 +	1.268e+03 +	1.639e+03 +	1.133e+03 ≈	1.151e+03 ≈	1.392e+03 +	1.195e+03 ≈	1.175e+03 ≈	1.458e+03 +	1.448e+03 +	**1.063e+03** −	1.167e+03
	std	4.918e+01	5.181e+01	4.983e+01	7.740e+01	2.591e+01	1.771e+01	3.409e+01	4.585e+01	3.570e+01	3.852e+01	5.505e+01	5.154e+01
f_9	mean	5.429e+04 +	2.308e+04 +	5.800e+04 +	1.099e+04 ≈	1.144e+04 ≈	2.558e+04 +	2.304e+04 +	1.290e+04 ≈	3.119e+04 +	3.245e+04 +	**1.018e+04** −	1.176e+04
	std	1.536e+03	2.468e+03	4.952e+03	6.122e+03	1.537e+03	2.472e+03	4.462e+03	3.087e+03	2.534e+03	4.121e+03	2.249e+03	1.278e+03
f_{10}	mean	1.539e+04 +	1.196e+04 +	1.580e+04 +	8.492e+03 +	9.536e+03 +	1.303e+04 +	1.015e+04 +	9.889e+03 +	1.408e+04 +	1.412e+04 +	8.268e+03 ≈	**7.829e+03**
	std	8.125e+02	2.000e+03	2.479e+02	2.187e+03	6.361e+02	5.201e+02	7.983e+02	2.248e+03	7.037e+02	4.803e+02	7.218e+02	9.960e+02
f_{11}	mean	2.964e+04 +	4.466e+03 +	3.494e+04 +	1.359e+03 ≈	1.391e+03 ≈	1.488e+04 +	3.155e+03 +	3.087e+04 +	1.687e+04 +	1.758e+04 +	**1.351e+03** −	1.413e+03
	std	5.834e+01	7.906e+01	6.274e+03	2.083e+03	2.752e+03	2.340e+03	1.229e+03	1.393e+04	4.076e+03	3.272e+03	5.882e+01	8.628e+01
f_{12}	mean	5.062e+10 +	1.714e+09 +	6.883e+10 +	2.966e+07 +	1.483e+07 +	1.765e+10 +	3.927e+09 +	1.484e+10 +	2.116e+10 +	2.296e+10 +	2.637e+07 +	**9.340e+06**
	std	2.175e+07	1.325e+07	9.142e+09	1.280e+09	1.006e+10	3.920e+09	3.151e+09	5.500e+09	6.194e+09	7.398e+09	1.688e+07	6.588e+06
f_{13}	mean	2.259e+10 +	5.809e+07 +	3.277e+10 +	2.002e+05 +	**6.226e+04** −	3.422e+09 +	2.222e+07 +	5.979e+09 +	6.874e+09 +	7.127e+09 +	1.209e+05 ≈	1.041e+05
	std	1.428e+05	9.375e+04	4.821e+09	1.195e+08	6.181e+09	2.496e+09	5.217e+07	3.334e+09	2.328e+09	2.556e+09	7.031e+04	5.998e+04

Table 16 continued

Func.		CS	WOA	HGSO	AVOA	AGTO	GJO	HBA	EVO	COA	ICOA	CCOA	MSICOA
f_{14}	mean	2.878e+07 +	2.503e+06 +	4.485e+07 +	7.130e+05 +	1.421e+05 ≈	5.070e+06 +	3.077e+05 ≈	1.919e+07 +	3.219e+06 +	3.163e+06 +	**1.318e+05** ≈	2.441e+05
	std	4.274e+05	4.639e+05	1.324e+07	4.809e+06	1.577e+07	3.901e+06	1.750e+05	1.793e+07	2.299e+06	2.056e+06	7.885e+04	1.863e+05
f_{15}	mean	5.925e+09 +	4.396e+05 ≈	8.794e+09 +	5.530e+04 ≈	4.106e+04 ≈	6.879e+08 +	3.933e+04 ≈	1.518e+09 +	5.975e+08 +	5.318e+08 +	**3.756e+04** ≈	6.597e+04
	std	2.794e+04	6.906e+04	2.120e+09	1.239e+06	2.337e+09	7.831e+08	3.504e+04	1.262e+09	4.390e+08	4.125e+08	1.468e+04	6.001e+04
f_{16}	mean	8.254e+03 +	5.964e+03 +	9.159e+03 +	4.044e+03 +	3.886e+03 ≈	4.931e+03 +	4.353e+03 +	5.360e+03 +	6.387e+03 +	6.384e+03 +	**3.520e+03** ≈	3.615e+03
	std	5.179e+02	5.319e+02	4.853e+02	1.802e+03	6.786e+02	3.824e+02	6.593e+02	5.914e+02	3.996e+02	4.757e+02	4.390e+02	4.792e+02
f_{17}	mean	1.118e+04 +	5.437e+03 +	1.592e+04 +	3.594e+03 ≈	3.523e+03 ≈	4.665e+03 +	3.716e+03 ≈	4.201e+03 +	4.735e+03 +	4.741e+03 +	**3.310e+03** ≈	3.574e+03
	std	4.313e+02	3.954e+02	4.292e+03	1.785e+03	5.522e+03	3.238e+02	3.571e+02	4.032e+02	4.512e+02	3.282e+02	3.911e+02	3.505e+02
f_{18}	mean	1.300e+08 +	5.545e+06 +	2.055e+08 +	3.156e+06 +	**5.322e+05** −	3.068e+07 +	3.316e+06 +	4.952e+07 +	1.785e+07 +	1.349e+07 +	1.187e+06 +	8.571e+05
	std	2.707e+06	4.701e+05	4.666e+07	4.835e+06	5.783e+07	2.082e+07	2.797e+06	2.612e+07	1.380e+07	6.948e+06	8.550e+05	4.654e+05
f_{19}	mean	2.630e+09 +	1.421e+05 ≈	3.949e+09 +	8.376e+04 ≈	**2.318e+04** −	5.991e+08 +	6.528e+04 ≈	5.723e+08 +	3.957e+08 +	4.191e+08 +	8.078e+05 +	1.154e+05
	std	3.604e+04	2.440e+04	9.103e+08	3.124e+05	8.243e+08	3.794e+08	2.794e+04	4.748e+08	1.565e+08	2.215e+08	6.221e+05	1.672e+05
f_{20}	mean	4.332e+03 +	3.748e+03 +	4.585e+03 +	3.594e+03 +	**3.167e+03** ≈	3.930e+03 +	3.400e+03 +	3.496e+03 +	3.808e+03 +	3.822e+03 +	3.393e+03 +	3.203e+03
	std	3.908e+02	3.624e+02	1.339e+02	2.183e+02	2.369e+02	2.085e+02	3.316e+02	4.378e+02	2.433e+02	2.763e+02	3.001e+02	2.660e+02
f_{21}	mean	3.160e+03 +	2.939e+03 +	3.272e+03 +	2.717e+03 ≈	2.639e+03 ≈	2.866e+03 +	2.783e+03 +	2.745e+03 +	3.003e+03 +	2.999e+03 +	**2.585e+03** −	2.673e+03
	std	6.692e+01	5.724e+01	7.804e+01	9.867e+01	4.437e+01	2.548e+01	7.496e+01	5.052e+01	4.458e+01	4.628e+01	4.091e+01	7.621e+01
f_{22}	mean	1.703e+04 +	1.378e+04 +	1.746e+04 +	1.051e+04 ≈	1.043e+04 ≈	1.070e+04 ≈	1.191e+04 +	1.127e+04 +	1.571e+04 +	1.582e+04 +	9.691e+03 ≈	**9.587e+03**
	std	1.098e+03	2.941e+03	3.661e+02	2.092e+03	5.094e+02	2.297e+03	9.163e+02	1.841e+03	6.130e+02	5.728e+02	1.050e+03	2.080e+03
f_{23}	mean	4.247e+03 +	4.050e+03 +	4.354e+03 +	3.383e+03 +	3.339e+03 +	3.527e+03 +	3.660e+03 +	3.445e+03 +	3.865e+03 +	3.883e+03 +	3.285e+03 +	**3.200e+03**
	std	1.553e+02	1.907e+02	8.974e+01	1.759e+02	1.333e+02	5.814e+01	1.774e+02	7.659e+01	1.110e+02	1.150e+02	1.063e+02	1.251e+02
f_{24}	mean	4.592e+03 +	4.110e+03 +	4.667e+03 +	3.567e+03 +	3.532e+03 +	3.725e+03 +	3.727e+03 +	3.635e+03 +	4.081e+03 +	4.028e+03 +	3.558e+03 +	**3.341e+03**
	std	1.529e+02	2.167e+02	1.283e+02	2.413e+02	1.655e+02	5.261e+01	1.746e+02	1.376e+02	1.999e+02	1.386e+02	1.413e+02	1.849e+02

Table 16 continued

Func.		CS	WOA	HGSO	AVOA	AGTO	GJO	HBA	EVO	COA	ICOA	CCOA	MSICOA
f_{25}	mean	2.046e+04 +	4.867e+03 +	1.823e+04 +	3.129e+03 +	3.167e+03 +	6.590e+03 +	4.518e+03 +	8.540e+03 +	1.304e+04 +	1.321e+04 +	3.100e+03 ≈	**3.090e+03**
	std	3.860e+01	6.662e+01	3.132e+03	7.018e+02	9.355e+02	6.454e+02	6.276e+02	1.311e+03	1.881e+03	1.727e+03	2.003e+01	2.374e+01
f_{26}	mean	1.913e+04 +	1.540e+04 +	1.927e+04 +	1.045e+04 +	8.275e+03 +	1.190e+04 +	1.272e+04 +	1.260e+04 +	1.445e+04 +	1.476e+04 +	9.278e+03 +	**6.770e+03**
	std	1.308e+03	3.369e+03	1.467e+03	1.597e+03	5.017e+02	4.492e+02	1.438e+03	1.053e+03	1.207e+03	1.406e+03	1.979e+03	3.544e+03
f_{27}	mean	6.114e+03 +	6.302e+03 +	6.240e+03 +	3.887e+03 +	4.705e+03 +	4.696e+03 +	4.269e+03 +	4.414e+03 +	4.512e+03 +	4.550e+03 +	4.309e+03 +	**3.557e+03**
	std	1.931e+02	6.205e+02	2.845e+02	9.919e+02	2.509e+02	2.005e+02	3.268e+02	3.039e+02	1.786e+02	1.827e+02	2.586e+02	1.213e+02
f_{28}	mean	1.346e+04 +	5.515e+03 +	1.486e+04 +	3.398e+03 +	3.446e+03 +	6.850e+03 +	5.234e+03 +	7.524e+03 +	1.012e+04 +	9.675e+03 +	3.493e+03 +	**3.345e+03**
	std	3.427e+01	7.202e+01	1.414e+03	5.930e+02	7.708e+02	5.025e+02	4.950e+02	6.710e+02	9.090e+02	9.527e+02	6.477e+01	3.383e+01
f_{29}	mean	2.183e+04 +	9.402e+03 +	3.018e+04 +	5.220e+03 +	6.005e+03 +	9.083e+03 +	6.937e+03 +	9.456e+03 +	9.060e+03 +	9.051e+03 +	5.686e+03 +	**4.978e+03**
	std	3.126e+02	1.860e+03	8.287e+03	1.633e+03	9.963e+03	1.126e+03	1.053e+03	2.925e+03	1.072e+03	1.079e+03	4.095e+02	3.968e+02
f_{30}	mean	4.500e+09 +	3.355e+07 +	6.470e+09 +	9.388e+06 +	**2.034e+06** −	1.352e+09 +	6.249e+07 +	1.249e+09 +	1.209e+09 +	1.342e+09 +	4.901e+07 +	3.598e+06
	std	2.785e+06	1.452e+06	1.069e+09	1.986e+07	1.042e+09	2.416e+08	2.599e+07	7.302e+08	4.942e+08	4.009e+08	8.565e+06	1.720e+06
+/≈/−		29/0/0	27/2/0	29/0/0	18/11/0	12/12/5	28/1/0	23/5/1	25/3/1	29/0/0	29/0/0	15/9/5	–
Avg. rank		7.2	11.0	11.8	3.4	2.8	7.4	5.2	7.0	8.6	8.8	2.4	**2.2**

Table 17 Experimental results in 100-D CEC2017

Func.		CS	WOA	HGSO	AVOA	AGTO	GJO	HBA	EVO	COA	ICOA	CCOA	MSICOA
f_1	mean	3.048e+11 +	7.722e+10 +	2.837e+11 +	**1.573e+06** −	6.293e+08 +	1.783e+11 +	8.487e+10 +	1.742e+11 +	2.432e+11 +	2.544e+11 +	1.735e+06 −	3.466e+06
	std	2.765e+06	1.561e+09	3.566e+10	1.944e+10	6.326e+09	6.505e+09	1.515e+10	1.741e+10	1.615e+10	1.458e+10	3.367e+06	1.825e+06
f_3	mean	6.190e+05 +	3.195e+05 +	7.787e+05 +	2.766e+05 ≈	**1.533e+05** −	3.465e+05 +	2.251e+05 −	5.879e+06 +	3.971e+05 +	4.210e+05 +	2.637e+05 ≈	2.759e+05
	std	1.806e+04	1.865e+04	7.704e+04	3.178e+04	8.834e+04	1.322e+04	2.152e+04	1.881e+07	4.263e+04	3.370e+04	1.340e+04	2.180e+04
f_4	mean	9.073e+04 +	1.015e+04 +	1.289e+05 +	8.378e+02 +	1.106e+03 +	2.922e+04 +	1.047e+04 +	3.775e+04 +	7.224e+04 +	7.256e+04 +	9.358e+02 +	**7.702e+02**
	std	7.122e+01	3.242e+02	2.002e+04	3.266e+03	1.315e+04	3.186e+03	2.438e+03	8.654e+03	1.320e+04	1.354e+04	1.057e+02	4.420e+01
f_5	mean	2.313e+03 +	1.669e+03 +	2.282e+03 +	1.334e+03 ≈	1.342e+03 ≈	1.835e+03 +	1.481e+03 +	1.565e+03 +	2.087e+03 +	2.082e+03 +	**1.189e+03** −	1.308e+03
	std	6.083e+01	6.977e+01	1.038e+02	1.677e+02	1.589e+01	3.107e+01	5.192e+01	5.591e+01	6.468e+01	5.963e+01	5.625e+01	6.436e+01
f_6	mean	7.262e+02 +	6.879e+02 +	7.283e+02 +	**6.550e+02** −	6.634e+02 +	6.949e+02 +	6.760e+02 +	6.593e+02 ≈	7.053e+02 +	7.064e+02 +	6.595e+02 ≈	6.593e+02
	std	3.466e+00	3.035e+00	6.266e+00	7.983e+00	1.601e+00	2.483e+00	3.365e+00	4.911e+00	4.321e+00	3.381e+00	3.634e+00	3.620e+00
f_7	mean	6.603e+03 +	3.503e+03 +	4.232e+03 +	2.853e+03 ≈	2.995e+03 ≈	3.354e+03 +	3.263e+03 +	3.539e+03 +	4.028e+03 +	4.028e+03 +	**2.194e+03** −	2.890e+03
	std	2.606e+02	1.711e+02	7.765e+02	1.984e+02	4.409e+01	8.963e+01	1.444e+02	2.175e+02	7.417e+01	7.860e+01	1.252e+02	2.602e+02
f_8	mean	2.700e+03 +	2.143e+03 +	2.768e+03 +	1.731e+03 ≈	1.746e+03 ≈	2.240e+03 +	1.879e+03 +	1.963e+03 +	2.512e+03 +	2.502e+03 +	**1.545e+03** −	1.778e+03
	std	9.981e+01	9.713e+01	9.438e+01	1.499e+02	3.145e+01	3.760e+01	8.038e+01	1.267e+02	6.466e+01	6.711e+01	7.670e+01	8.371e+01
f_9	mean	1.312e+05 +	4.278e+04 +	1.093e+05 +	2.340e+04 ≈	2.488e+04 +	6.524e+04 +	4.920e+04 +	3.794e+04 +	7.629e+04 +	7.736e+04 +	2.335e+04 ≈	**2.280e+04**
	std	1.663e+03	8.794e+02	1.521e+04	8.823e+03	1.808e+03	4.664e+03	1.137e+04	1.943e+04	4.335e+03	5.418e+03	2.263e+03	1.528e+03
f_{10}	mean	3.225e+04 +	2.911e+04 +	3.323e+04 +	1.587e+04 ≈	1.977e+04 +	2.822e+04 +	2.098e+04 +	1.999e+04 +	3.106e+04 +	3.070e+04 +	1.545e+04 ≈	**1.520e+04**
	std	1.769e+03	4.280e+03	4.623e+02	2.731e+03	5.726e+02	9.431e+02	2.279e+03	3.486e+03	8.871e+02	6.310e+02	1.850e+03	1.443e+03
f_{11}	mean	2.420e+05 +	5.817e+04 +	3.449e+05 +	8.349e+03 ≈	9.175e+03 ≈	1.691e+05 +	2.580e+04 +	4.100e+05 +	2.056e+05 +	1.841e+05 +	2.446e+04 +	**7.641e+03**
	std	3.428e+03	5.313e+03	3.582e+04	1.899e+04	3.438e+04	1.471e+04	6.995e+03	1.484e+05	3.662e+04	2.930e+04	1.094e+04	2.661e+03
f_{12}	mean	1.581e+11 +	1.168e+10 +	2.101e+11 +	1.138e+08 +	1.243e+08 +	7.741e+10 +	2.247e+10 +	6.508e+10 +	1.201e+11 +	1.195e+11 +	1.023e+08 +	**5.288e+07**
	std	6.559e+07	1.214e+08	2.648e+10	7.559e+09	1.578e+10	8.652e+09	9.682e+09	1.823e+10	1.370e+10	1.964e+10	3.813e+07	2.943e+07
f_{13}	mean	3.505e+10 +	5.440e+08 +	4.624e+10 +	7.368e+04 ≈	1.909e+05 +	1.443e+10 +	2.575e+09 +	1.394e+10 +	2.030e+10 +	2.071e+10 +	**6.629e+04** ≈	7.598e+04
	std	3.730e+04	6.638e+05	5.577e+09	7.633e+08	3.821e+09	2.043e+09	1.940e+09	5.638e+09	4.532e+09	5.146e+09	1.414e+04	3.605e+04
f_{14}	mean	1.192e+08 +	1.796e+06 +	1.679e+08 +	1.108e+06 +	6.050e+05 ≈	3.025e+07 +	3.011e+06 +	3.399e+07 +	3.086e+07 +	2.747e+07 +	**4.943e+05** −	8.035e+05

Table 17 continued

Func.		CS	WOA	HGSO	AVOA	AGTO	GJO	HBA	EVO	COA	ICOA	CCOA	MSICOA
	std	4.881e+05	2.514e+05	3.256e+07	1.177e+06	3.767e+07	1.318e+07	1.398e+06	1.800e+07	1.288e+07	1.321e+07	2.460e+05	3.901e+05
f_{15}	mean	1.545e+10 +	1.446e+07 +	2.173e+10 +	5.657e+04 ≈	**2.553e+04** −	5.443e+09 +	3.274e+08 +	4.642e+09 +	5.567e+09 +	5.359e+09 +	4.830e+04 ≈	5.618e+04
	std	2.672e+04	2.397e+04	3.591e+09	3.490e+07	2.243e+09	1.422e+09	7.667e+08	2.474e+09	2.330e+09	2.178e+09	1.521e+04	2.910e+04
f_{16}	mean	1.937e+04 +	1.285e+04 +	2.322e+04 +	6.484e+03 +	**6.198e+03** ≈	1.266e+04 +	9.024e+03 +	1.198e+04 +	1.499e+04 +	1.517e+04 +	6.441e+03 +	6.217e+03
	std	8.474e+02	9.515e+02	1.275e+03	4.138e+03	1.350e+03	5.923e+02	1.383e+03	1.454e+03	1.138e+03	1.456e+03	5.603e+02	8.360e+02
f_{17}	mean	1.113e+06 +	1.905e+04 +	2.993e+06 +	**5.748e+03** ≈	6.227e+03 ≈	3.118e+04 +	9.183e+03 +	7.238e+04 +	6.808e+04 +	4.583e+04 +	5.806e+03 ≈	6.130e+03
	std	6.896e+02	7.784e+02	7.405e+05	2.825e+04	1.718e+06	2.143e+04	2.652e+03	7.927e+04	7.075e+04	3.456e+04	4.899e+02	6.853e+02
f_{18}	mean	2.048e+08 +	3.132e+06 +	3.231e+08 +	1.551e+06 ≈	9.712e+05 −	4.623e+07 +	4.654e+06 +	5.056e+07 +	3.161e+07 +	4.304e+07 +	**8.771e+05** −	1.812e+06
	std	6.508e+05	6.217e+05	6.402e+07	1.568e+06	8.304e+07	1.651e+07	2.170e+06	4.004e+07	1.502e+07	1.751e+07	4.281e+05	7.826e+05
f_{19}	mean	1.562e+10 +	8.381e+07 +	2.242e+10 +	2.815e+05 +	**3.048e+04** ≈	4.751e+09 +	6.438e+07 +	5.114e+09 +	6.478e+09 +	5.864e+09 +	3.441e+06 +	1.199e+05
	std	1.857e+05	3.718e+04	3.085e+09	2.570e+08	3.355e+09	1.054e+09	8.289e+07	2.581e+09	2.484e+09	1.799e+09	1.203e+06	1.470e+05
f_{20}	mean	7.877e+03 +	6.782e+03 +	8.250e+03 +	5.514e+03 +	5.420e+03 +	7.143e+03 +	5.715e+03 +	6.738e+03 +	7.176e+03 +	7.129e+03 +	5.460e+03 +	**5.186e+03**
	std	4.128e+02	4.621e+02	1.881e+02	6.149e+02	2.918e+02	4.220e+02	4.011e+02	1.372e+03	3.881e+02	3.847e+02	4.455e+02	5.342e+02
f_{21}	mean	4.604e+03 +	4.133e+03 +	4.811e+03 +	3.566e+03 +	3.431e+03 ≈	3.929e+03 +	3.878e+03 +	3.628e+03 +	4.252e+03 +	4.287e+03 +	**3.326e+03** ≈	3.384e+03
	std	2.048e+02	1.488e+02	7.428e+01	2.002e+02	9.785e+01	4.609e+01	2.221e+02	1.214e+02	1.036e+02	1.074e+02	1.287e+02	1.595e+02
f_{22}	mean	3.504e+04 +	3.057e+04 +	3.552e+04 +	1.951e+04 ≈	2.249e+04 +	3.075e+04 +	2.452e+04 +	2.555e+04 +	3.323e+04 +	3.301e+04 +	**1.904e+04** ≈	1.911e+04
	std	1.688e+03	2.950e+03	3.878e+02	2.818e+03	5.840e+02	2.904e+03	1.585e+03	6.299e+03	4.783e+02	7.994e+02	1.230e+03	1.673e+03
f_{23}	mean	6.279e+03 +	5.858e+03 +	6.448e+03 +	4.140e+03 +	4.229e+03 +	5.184e+03 +	5.009e+03 +	4.559e+03 +	5.779e+03 +	5.612e+03 +	4.499e+03 +	**3.886e+03**
	std	1.850e+02	2.326e+02	1.964e+02	4.238e+02	2.616e+02	1.540e+02	2.973e+02	1.592e+02	3.066e+02	3.042e+02	1.985e+02	2.284e+02
f_{24}	mean	9.858e+03 +	8.319e+03 +	1.062e+04 +	5.095e+03 +	5.807e+03 +	7.124e+03 +	6.438e+03 +	5.877e+03 +	7.948e+03 +	7.814e+03 +	5.878e+03 +	**4.544e+03**
	std	3.376e+02	1.736e+03	5.837e+02	7.955e+02	4.193e+02	3.468e+02	6.153e+02	3.364e+02	4.734e+02	5.731e+02	3.655e+02	2.443e+02
f_{25}	mean	3.938e+04 +	8.750e+03 +	3.314e+04 +	3.475e+03 +	3.767e+03 +	1.427e+04 +	8.457e+03 +	1.846e+04 +	2.826e+04 +	2.880e+04 +	3.610e+03 +	**3.396e+03**
	std	5.758e+01	1.560e+02	8.304e+03	1.943e+03	1.089e+03	9.560e+02	1.820e+03	2.518e+03	2.855e+03	2.358e+03	5.512e+01	4.902e+01

Table 17 continued

Func.		CS	WOA	HGSO	AVOA	AGTO	GJO	HBA	EVO	COA	ICOA	CCOA	MSICOA
f_{26}	mean	5.544e+04 +	3.485e+04 +	5.998e+04 +	2.305e+04 +	2.484e+04 +	3.451e+04 +	3.327e+04 +	3.447e+04 +	4.098e+04 +	4.169e+04 +	2.600e+04 +	**1.755e+04**
	std	2.773e+03	5.150e+03	3.400e+03	3.430e+03	3.313e+03	1.168e+03	2.991e+03	3.378e+03	3.856e+03	4.937e+03	3.254e+03	5.590e+03
f_{27}	mean	1.144e+04 +	9.509e+03 +	1.213e+04 +	4.070e+03 +	5.774e+03 +	7.692e+03 +	5.494e+03 +	5.753e+03 +	7.319e+03 +	6.972e+03 +	5.194e+03 +	**3.646e+03**
	std	2.832e+02	2.106e+03	5.678e+02	1.630e+03	6.154e+02	4.152e+02	6.475e+02	3.964e+02	5.034e+02	5.609e+02	3.671e+02	1.019e+02
f_{28}	mean	3.729e+04 +	9.574e+03 +	4.029e+04 +	3.553e+03 +	3.843e+03 +	1.908e+04 +	1.179e+04 +	2.269e+04 +	2.998e+04 +	2.798e+04 +	4.354e+03 +	**3.513e+03**
	std	2.663e+01	1.837e+02	3.930e+03	1.084e+03	1.157e+03	8.901e+02	2.372e+03	2.022e+03	1.325e+03	2.547e+03	2.590e+02	3.836e+01
f_{29}	mean	1.769e+05 +	1.905e+04 +	4.443e+05 +	8.053e+03 +	8.415e+03 +	3.308e+04 +	1.348e+04 +	2.184e+04 +	3.637e+04 +	3.553e+04 +	9.915e+03 +	**7.285e+03**
	std	5.317e+02	8.756e+02	9.409e+04	5.174e+03	1.673e+05	1.159e+04	1.965e+03	9.791e+03	1.038e+04	1.206e+04	7.074e+02	7.435e+02
f_{30}	mean	2.656e+10 +	1.706e+08 +	3.700e+10 +	4.353e+06 +	**8.135e+05** −	1.375e+10 +	2.520e+09 +	1.156e+10 +	9.874e+09 +	1.215e+10 +	2.035e+07 +	2.537e+06
	std	2.042e+06	8.053e+05	3.981e+09	3.001e+08	3.760e+09	1.882e+09	2.222e+09	4.541e+09	2.541e+09	3.529e+09	1.070e+07	2.644e+06
+/≈/−		29/0/0	29/0/0	29/0/0	15/12/2	16/9/4	29/0/0	28/0/1	28/1/0	29/0/0	29/0/0	14/9/6	–
Avg. rank		6.6	11.1	11.8	2.6	3.1	7.7	5.4	7.0	9.2	8.9	2.6	**2.0**

Table 18 The p values between MSICOA and competitor optimizers in 50-D CEC2017

Func	CS	WOA	HGSO	AVOA	AGTO	GJO	HBA	EVO	COA	ICOA	CCOA	MSICOA
f_1	6.796e−08	6.796e−08	6.796e−08	6.220e−04	6.796e−08	6.796e−08	6.796e−08	6.796e−08	6.796e−08	6.796e−08	7.898e−08	–
f_3	6.796e−08	6.220e−04	6.796e−08	1.014e−03	1.431e−07	9.173e−08	3.639e−03	6.796e−08	6.796e−08	1.065e−07	2.184e−03	–
f_4	6.796e−08	6.796e−08	6.796e−08	5.310e−03	1.625e−03	6.796e−08	6.796e−08	6.796e−08	6.796e−08	6.796e−08	2.564e−02	–
f_5	6.796e−08	1.657e−07	6.796e−08	4.570e−01	4.094e−01	6.796e−08	4.703e−03	3.369e−01	6.796e−08	6.796e−08	3.499e−06	–
f_6	6.796e−08	6.796e−08	6.796e−08	2.733e−01	2.748e−02	6.796e−08	1.657e−07	2.139e−03	6.796e−08	6.796e−08	1.719e−01	–
f_7	6.796e−08	2.563e−07	6.796e−08	1.264e−01	2.616e−01	7.579e−04	4.680e−05	1.807e−05	6.796e−08	6.796e−08	4.539e−07	–
f_8	6.796e−08	3.293e−05	6.796e−08	3.851e−01	5.428e−01	6.796e−08	4.388e−01	6.359e−01	6.796e−08	6.796e−08	3.987e−06	–
f_9	6.796e−08	1.235e−07	6.796e−08	7.205e−02	5.250e−01	6.796e−08	6.796e−08	2.393e−01	6.796e−08	6.796e−08	3.057e−03	–
f_{10}	6.796e−08	2.218e−07	6.796e−08	2.944e−02	2.799e−03	6.796e−08	2.563e−07	1.037e−04	6.796e−08	6.796e−08	1.895e−01	–
f_{11}	6.796e−08	6.796e−08	6.796e−08	6.787e−02	5.250e−01	6.796e−08	6.796e−08	6.796e−08	6.796e−08	6.796e−08	1.667e−02	–
f_{12}	6.796e−08	6.796e−08	6.796e−08	1.444e−04	1.556e−02	6.796e−08	6.796e−08	6.796e−08	6.796e−08	6.796e−08	3.705e−05	–
f_{13}	6.796e−08	1.415e−05	6.796e−08	1.143e−02	4.155e−04	6.796e−08	6.796e−08	6.796e−08	6.796e−08	6.796e−08	2.977e−01	–
f_{14}	6.796e−08	4.166e−05	6.796e−08	1.794e−01	7.406e−05	9.173e−08	1.895e−01	6.796e−08	6.796e−08	2.563e−07	8.103e−02	–
f_{15}	6.796e−08	1.404e−01	6.796e−08	8.181e−01	2.748e−01	6.796e−08	2.184e−01	6.796e−08	6.796e−08	6.796e−08	3.507e−01	–
f_{16}	6.796e−08	3.939e−07	6.796e−08	1.143e−02	1.199e−01	1.431e−07	1.014e−03	1.235e−07	6.796e−08	6.796e−08	6.359e−01	–
f_{17}	6.796e−08	1.431e−07	6.796e−08	7.557e−01	5.428e−01	9.173e−08	1.895e−01	5.896e−05	1.657e−07	7.898e−08	6.389e−02	–
f_{18}	6.796e−08	1.807e−05	6.796e−08	5.091e−04	1.332e−02	6.796e−08	7.406e−05	6.796e−08	6.796e−08	7.898e−08	2.853e−02	–
f_{19}	6.796e−08	7.150e−01	6.796e−08	5.652e−02	1.997e−04	6.796e−08	3.793e−01	6.796e−08	6.796e−08	6.796e−08	1.600e−05	–
f_{20}	6.796e−08	2.356e−06	6.796e−08	2.341e−03	5.428e−01	1.235e−07	3.103e−02	2.564e−02	1.201e−06	1.803e−06	7.643e−03	–
f_{21}	6.796e−08	1.065e−07	6.796e−08	4.986e−01	3.104e−01	1.065e−07	3.048e−04	2.139e−03	6.796e−08	6.796e−08	2.745e−04	–
f_{22}	6.796e−08	6.015e−07	6.796e−08	2.503e−01	7.643e−02	5.609e−01	9.748e−06	8.355e−03	6.796e−08	6.796e−08	4.735e−01	–
f_{23}	6.796e−08	6.796e−08	6.796e−08	7.579e−04	7.712e−03	1.918e−07	1.431e−07	3.069e−06	6.796e−08	6.796e−08	2.564e−02	–
f_{24}	6.796e−08	1.065e−07	6.796e−08	3.750e−04	2.561e−03	1.201e−06	7.577e−06	2.925e−05	1.235e−07	7.898e−08	4.155e−04	–

Table 18 continued

Func	CS	WOA	HGSO	AVOA	AGTO	GJO	HBA	EVO	COA	ICOA	CCOA	MSICOA
f_{25}	6.796e−08	6.796e−08	6.796e−08	6.868e−04	1.803e−06	6.796e−08	6.796e−08	6.796e−08	6.796e−08	6.796e−08	1.636e−01	–
f_{26}	6.796e−08	6.796e−08	6.796e−08	8.357e−04	3.205e−02	9.173e−08	1.047e−06	1.065e−07	6.796e−08	6.796e−08	3.372e−02	–
f_{27}	6.796e−08	6.796e−08	6.796e−08	4.540e−06	7.898e−08	6.796e−08	1.431e−07	7.898e−08	6.796e−08	6.796e−08	6.796e−08	–
f_{28}	6.796e−08	6.796e−08	6.796e−08	5.255e−05	2.302e−05	6.796e−08	6.796e−08	6.796e−08	6.796e−08	6.796e−08	2.218e−07	–
f_{29}	6.796e−08	6.796e−08	6.796e−08	5.652e−03	8.355e−03	6.796e−08	1.065e−07	6.796e−08	6.796e−08	6.796e−08	3.293e−05	–
f_{30}	6.796e−08	6.796e−08	6.796e−08	4.539e−07	1.481e−03	6.796e−08	6.796e−08	6.796e−08	6.796e−08	6.796e−08	6.796e−08	–

Table 19 The p values between MSICOA and competitor optimizers in 100-D CEC2017

Func	CS	WOA	HGSO	AVOA	AGTO	GJO	HBA	EVO	COA	ICOA	CCOA	MSICOA
f_1	6.796e−08	6.796e−08	6.796e−08	9.209e−04	6.796e−08	6.796e−08	6.796e−08	6.796e−08	6.796e−08	6.796e−08	8.597e−06	–
f_3	6.796e−08	5.896e−05	6.796e−08	7.764e−01	6.796e−08	6.796e−08	9.127e−07	6.796e−08	9.173e−08	6.796e−08	6.389e−02	–
f_4	6.796e−08	6.796e−08	6.796e−08	2.561e−03	6.796e−08	6.796e−08	6.796e−08	6.796e−08	6.796e−08	6.796e−08	5.166e−06	–
f_5	6.796e−08	1.431e−07	6.796e−08	1.636e−01	1.895e−01	6.796e−08	5.227e−07	7.898e−08	6.796e−08	6.796e−08	3.987e−06	–
f_6	6.796e−08	6.796e−08	6.796e−08	1.227e−03	1.227e−03	6.796e−08	6.796e−08	9.461e−01	6.796e−08	6.796e−08	9.676e−01	–
f_7	6.796e−08	2.218e−07	6.796e−08	6.359e−01	3.235e−01	9.173e−08	8.597e−06	1.657e−07	6.796e−08	6.796e−08	9.173e−08	–
f_8	6.796e−08	1.918e−07	6.796e−08	8.585e−02	2.853e−01	6.796e−08	7.579e−04	9.748e−06	6.796e−08	6.796e−08	7.948e−07	–
f_9	6.796e−08	6.796e−08	6.796e−08	5.792e−01	1.251e−05	6.796e−08	6.796e−08	9.173e−08	6.796e−08	6.796e−08	1.988e−01	–
f_{10}	6.796e−08	6.796e−08	6.796e−08	2.287e−01	4.540e−06	6.796e−08	1.235e−07	1.918e−07	6.796e−08	6.796e−08	6.949e−01	–
f_{11}	6.796e−08	6.796e−08	6.796e−08	6.168e−01	5.792e−01	6.796e−08	6.796e−08	6.796e−08	6.796e−08	6.796e−08	1.657e−07	–
f_{12}	6.796e−08	6.796e−08	6.796e−08	1.782e−03	4.679e−02	6.796e−08	6.796e−08	6.796e−08	6.796e−08	6.796e−08	1.159e−04	–
f_{13}	6.796e−08	6.796e−08	6.796e−08	6.750e−01	9.209e−04	6.796e−08	6.796e−08	6.796e−08	6.796e−08	6.796e−08	5.792e−01	–
f_{14}	6.796e−08	2.222e−04	6.796e−08	1.058e−02	1.075e−01	6.796e−08	1.918e−07	6.796e−08	6.796e−08	6.796e−08	3.639e−03	–
f_{15}	6.796e−08	1.159e−04	6.796e−08	1.000e+00	1.610e−04	6.796e−08	6.796e−08	6.796e−08	6.796e−08	6.796e−08	5.250e−01	–
f_{16}	6.796e−08	1.657e−07	6.796e−08	3.942e−02	1.000e+00	6.796e−08	2.960e−07	6.796e−08	6.796e−08	6.796e−08	2.616e−01	–
f_{17}	6.796e−08	1.918e−07	6.796e−08	1.636e−01	6.750e−01	6.796e−08	3.705e−05	6.796e−08	6.796e−08	6.796e−08	1.719e−01	–
f_{18}	6.796e−08	2.561e−03	6.796e−08	3.104e−01	5.629e−04	6.796e−08	4.166e−05	6.796e−08	6.796e−08	6.796e−08	6.610e−05	–
f_{19}	6.796e−08	2.563e−07	6.796e−08	5.091e−04	6.787e−02	6.796e−08	6.796e−08	6.796e−08	6.796e−08	6.796e−08	6.796e−08	–
f_{20}	6.796e−08	1.201e−06	6.796e−08	1.143e−02	2.310e−02	1.657e−07	3.382e−04	2.596e−05	9.173e−08	1.065e−07	2.944e−02	–
f_{21}	6.796e−08	6.796e−08	6.796e−08	6.040e−03	4.407e−01	6.796e−08	2.218e−07	5.896e−05	6.796e−08	6.796e−08	2.503e−01	–
f_{22}	6.796e−08	6.796e−08	6.796e−08	6.168e−01	8.292e−05	6.796e−08	1.235e−07	7.577e−06	6.796e−08	6.796e−08	7.150e−01	–
f_{23}	6.796e−08	6.796e−08	6.796e−08	1.227e−03	1.444e−04	6.796e−08	6.796e−08	9.173e−08	6.796e−08	6.796e−08	1.235e−07	–
f_{24}	6.796e−08	6.796e−08	6.796e−08	7.577e−06	5.255e−05	6.796e−08	6.796e−08	6.796e−08	6.796e−08	6.796e−08	6.796e−08	–

Table 19 continued

Func	CS	WOA	HGSO	AVOA	AGTO	GJO	HBA	EVO	COA	ICOA	CCOA	MSICOA
f_{25}	6.796e−08	6.796e−08	6.796e−08	1.610e−04	6.796e−08	6.796e−08	6.796e−08	6.796e−08	6.796e−08	6.796e−08	6.796e−08	–
f_{26}	6.796e−08	6.796e−08	6.796e−08	4.601e−04	3.705e−05	6.796e−08	6.796e−08	6.796e−08	6.796e−08	6.796e−08	1.576e−06	–
f_{27}	6.796e−08	6.796e−08	6.796e−08	1.376e−06	3.416e−07	6.796e−08	6.796e−08	6.796e−08	6.796e−08	6.796e−08	6.796e−08	–
f_{28}	6.796e−08	6.796e−08	6.796e−08	6.868e−04	6.796e−08	6.796e−08	6.796e−08	6.796e−08	6.796e−08	6.796e−08	6.796e−08	–
f_{29}	6.796e−08	6.796e−08	6.796e−08	6.868e−04	3.382e−04	6.796e−08	6.796e−08	6.796e−08	6.796e−08	6.796e−08	9.173e−08	–
f_{30}	6.796e−08	6.796e−08	6.796e−08	1.116e−03	1.481e−03	6.796e−08	6.796e−08	6.796e−08	6.796e−08	6.796e−08	1.065e−07	–

B: Experimental results in CEC2020

Tables 20 and 21 summarize the detailed experimental results in CEC2020, while the p values between MSICOA and competitor algorithms are summarized in Tables 22 and 23.

Table 20 Experimental results in 10-D CEC2020

Func.		CS	WOA	HGSO	AVOA	AGTO	GJO	HBA	EVO	COA	ICOA	CCOA	MSICOA
f_1	mean	6.429e+09 +	1.022e+08 +	7.801e+09 +	3.446e+03 ≈	**1.857e+03** ≈	6.386e+08 +	1.010e+06 +	1.237e+09 +	1.346e+09 +	1.089e+09 +	1.840e+05 +	2.815e+03
	std	3.266e+03	2.676e+03	1.748e+09	1.843e+08	2.401e+09	2.454e+08	8.868e+05	1.028e+09	6.476e+08	5.813e+08	9.257e+04	2.465e+03
f_2	mean	5.225e+11 +	8.808e+09 +	6.207e+11 +	**3.508e+05** ≈	3.638e+05 ≈	6.018e+10 +	1.156e+09 +	8.888e+10 +	1.200e+11 +	1.134e+11 +	5.794e+06 +	5.671e+05
	std	3.617e+05	2.784e+05	2.102e+11	1.528e+10	1.769e+11	3.088e+10	3.708e+09	1.013e+11	7.056e+10	6.693e+10	3.660e+06	4.521e+05
f_3	mean	1.951e+11 +	5.823e+09 +	2.112e+11 +	2.048e+05 ≈	**1.838e+05** −	1.853e+10 +	4.925e+07 +	2.063e+10 +	4.156e+10 +	3.968e+10 +	4.928e+06 +	2.076e+05
	std	5.944e+05	1.854e+05	7.733e+10	1.685e+10	6.734e+10	1.572e+10	5.417e+07	2.255e+10	1.636e+10	1.585e+10	2.625e+06	2.281e+05
f_4	mean	5.338e+03 +	2.098e+03 +	1.055e+04 +	1.903e+03 ≈	1.904e+03 +	1.911e+03 +	1.906e+03 +	2.053e+03 +	2.000e+03 +	1.978e+03 +	**1.902e+03** ≈	1.903e+03
	std	1.517e+00	1.793e+00	3.312e+03	3.204e+02	8.109e+03	1.777e+01	5.596e+00	2.995e+02	2.109e+02	9.311e+01	5.431e−01	2.037e+00
f_5	mean	1.069e+06 +	1.728e+04 ≈	1.971e+06 +	2.944e+04 +	**6.467e+03** ≈	1.941e+05 +	1.473e+04 ≈	2.067e+05 +	4.340e+04 +	3.138e+04 +	2.201e+04 +	1.377e+04
	std	1.600e+04	4.282e+03	9.616e+05	2.463e+04	1.613e+06	1.177e+05	7.517e+03	4.733e+05	2.497e+04	1.872e+04	1.097e+04	1.125e+04
f_6	mean	3.570e+04 +	9.810e+03 +	5.509e+04 +	5.498e+03 +	**1.815e+03** −	5.288e+03 +	2.865e+03 ≈	1.192e+04 +	3.748e+03 +	4.028e+03 +	3.842e+03 +	2.686e+03
	std	4.936e+03	2.823e+02	2.510e+04	7.817e+03	4.451e+04	2.274e+03	1.494e+03	1.342e+04	1.551e+03	1.409e+03	2.807e+03	1.582e+03
f_7	mean	1.649e+06 +	2.944e+04 +	2.302e+06 +	2.508e+04 +	**7.753e+03** ≈	7.516e+04 +	2.046e+04 +	7.510e+04 +	4.503e+04 +	6.382e+04 +	2.137e+04 +	1.492e+04
	std	1.381e+04	6.580e+03	9.868e+05	2.226e+04	1.189e+06	4.745e+04	1.088e+04	1.468e+05	3.400e+04	6.009e+04	1.362e+04	1.481e+04
f_8	mean	2.344e+03 +	2.328e+03 +	2.352e+03 +	2.307e+03 +	2.306e+03 ≈	2.308e+03 +	2.311e+03 +	2.316e+03 +	2.321e+03 +	2.324e+03 +	**2.304e+03** ≈	2.305e+03
	std	3.754e+00	2.554e+00	1.021e+01	1.326e+01	9.036e+00	2.838e+00	6.348e+00	4.577e+00	4.258e+00	5.987e+00	1.880e+00	2.345e+00
f_9	mean	6.323e+03 +	2.984e+03 +	6.865e+03 +	2.590e+03 +	2.585e+03 +	3.196e+03 +	2.639e+03 +	3.899e+03 +	4.240e+03 +	4.165e+03 +	2.589e+03 +	**2.560e+03**
	std	3.001e+01	6.416e+01	7.570e+02	4.038e+02	9.828e+02	1.543e+02	5.783e+01	5.297e+02	3.104e+02	3.748e+02	5.564e+01	4.899e+01
f_{10}	mean	3.348e+03 +	3.173e+03 +	3.409e+03 +	3.012e+03 +	3.015e+03 +	3.023e+03 +	3.005e+03 +	3.111e+03 +	3.076e+03 +	3.061e+03 +	3.003e+03 +	**2.999e+03**
	std	3.545e+01	3.656e+01	1.098e+02	8.177e+01	1.311e+02	2.099e+01	2.713e+01	4.327e+01	3.813e+01	2.967e+01	3.093e+01	3.462e+01
+/≈/−		10/0/0	9/1/0	10/0/0	6/4/0	3/5/2	10/0/0	8/2/0	10/0/0	10/0/0	10/0/0	8/2/0	–
Avg. rank		7.3	11.0	12.0	4.0	2.1	7.1	4.3	8.7	8.3	7.9	3.3	**2.0**

Table 21 Experimental results in 20-D CEC2020

Func.		CS	WOA	HGSO	AVOA	AGTO	GJO	HBA	EVO	COA	ICOA	CCOA	MSICOA
f_1	mean	2.746e+10 +	2.251e+09 +	2.889e+10 +	**2.167e+03** −	4.649e+05 +	7.483e+09 +	1.625e+09 +	6.360e+09 +	9.330e+09 +	1.039e+10 +	2.938e+05 +	6.325e+03
	std	2.887e+03	9.457e+05	4.575e+09	1.862e+09	5.871e+09	1.609e+09	1.604e+09	2.563e+09	2.370e+09	3.217e+09	8.659e+04	4.129e+03
f_2	mean	2.566e+12 +	2.116e+11 +	2.834e+12 +	**5.788e+05** ≈	5.308e+06 +	5.105e+11 +	1.048e+11 +	5.078e+11 +	1.110e+12 +	1.058e+12 +	2.626e+07 +	7.174e+05
	std	6.406e+05	8.177e+06	4.513e+11	1.607e+11	4.150e+11	2.003e+11	1.004e+11	2.084e+11	3.645e+11	3.050e+11	8.313e+06	7.290e+05
f_3	mean	8.466e+11 +	8.452e+10 +	7.939e+11 +	3.468e+05 ≈	2.031e+06 +	1.763e+11 +	3.919e+10 +	1.648e+11 +	3.236e+11 +	2.910e+11 +	1.040e+07 +	**3.366e+05**
	std	5.520e+05	4.098e+06	1.910e+11	8.023e+10	1.204e+11	5.505e+10	4.961e+10	5.747e+10	8.843e+10	8.459e+10	4.083e+06	3.599e+05
f_4	mean	1.233e+05 +	3.387e+03 +	1.179e+05 +	1.910e+03 +	1.919e+03 +	2.056e+03 +	1.982e+03 +	2.982e+03 +	7.457e+03 +	5.670e+03 +	1.907e+03 ≈	**1.906e+03**
	std	3.389e+00	7.088e+00	7.333e+04	1.154e+03	4.408e+04	1.221e+02	8.600e+01	1.463e+03	6.440e+03	2.107e+03	1.694e+00	1.580e+00
f_5	mean	2.624e+07 +	9.511e+05 ≈	3.946e+07 +	3.278e+05 ≈	**1.937e+05** −	7.337e+06 +	3.093e+05 ≈	1.346e+07 +	2.958e+06 +	2.291e+06 +	2.163e+05 ≈	3.627e+05
	std	3.744e+05	3.281e+05	1.411e+07	2.037e+06	1.325e+07	6.073e+06	2.264e+05	1.451e+07	1.548e+06	1.099e+06	2.327e+05	4.521e+05
f_6	mean	1.300e+07 +	1.138e+04 +	2.675e+07 +	1.158e+04 +	6.801e+03 +	1.883e+06 +	6.635e+03 +	1.337e+07 +	7.735e+04 +	7.418e+04 +	8.402e+03 +	**2.951e+03**
	std	7.090e+03	1.530e+04	9.643e+06	6.872e+03	1.758e+07	3.957e+06	3.374e+03	2.369e+07	4.484e+04	5.611e+04	4.337e+03	1.101e+03
f_7	mean	7.601e+07 +	3.657e+05 +	9.292e+07 +	3.953e+04 ≈	5.407e+04 +	7.022e+06 +	**3.077e+04** ≈	2.041e+07 +	3.139e+06 +	2.893e+06 +	5.088e+04 +	3.520e+04
	std	2.343e+04	1.325e+05	2.792e+07	6.509e+05	5.179e+07	7.773e+06	1.920e+04	2.849e+07	2.545e+06	1.818e+06	2.588e+04	6.211e+04
f_8	mean	2.736e+03 +	2.512e+03 +	2.832e+03 +	2.336e+03 ≈	2.339e+03 +	2.372e+03 +	2.367e+03 +	2.384e+03 +	2.458e+03 +	2.472e+03 +	2.342e+03 +	**2.334e+03**
	std	5.858e+00	5.989e+00	1.046e+02	1.177e+02	1.435e+02	1.822e+01	2.781e+01	2.909e+01	3.541e+01	5.343e+01	9.093e+00	2.833e+00
f_9	mean	1.902e+04 +	6.890e+03 +	2.181e+04 +	2.619e+03 +	2.693e+03 +	8.586e+03 +	6.279e+03 +	9.263e+03 +	1.043e+04 +	1.099e+04 +	2.656e+03 +	**2.618e+03**
	std	8.400e+01	1.731e+02	3.181e+03	2.387e+03	2.227e+03	1.284e+03	1.914e+03	2.447e+03	1.736e+03	1.644e+03	5.811e+01	7.488e+01
f_{10}	mean	7.840e+03 +	3.940e+03 +	9.781e+03 +	3.288e+03 +	3.263e+03 +	3.890e+03 +	3.354e+03 +	4.783e+03 +	4.549e+03 +	4.522e+03 +	3.299e+03 +	**3.200e+03**
	std	9.954e+01	7.481e+01	1.194e+03	6.285e+02	1.000e+03	3.531e+02	2.284e+02	4.010e+02	4.557e+02	4.688e+02	1.071e+02	5.829e+01
+/≈/−		10/0/0	9/1/0	10/0/0	4/5/1	9/0/1	10/0/0	8/2/0	10/0/0	10/0/0	10/0/0	8/2/0	–
Avg. rank		6.6	11.1	11.8	2.7	3.2	7.6	4.1	8.4	8.9	8.5	3.4	**1.7**

Table 22 The p values between MSICOA and competitor optimizers in 10-D CEC2020

Func	CS	WOA	HGSO	AVOA	AGTO	GJO	HBA	EVO	COA	ICOA	CCOA	MSICOA
f_1	6.796e−08	6.796e−08	6.796e−08	9.461e−01	1.988e−01	6.796e−08	6.796e−08	6.796e−08	6.796e−08	6.796e−08	6.796e−08	–
f_2	6.796e−08	6.796e−08	6.796e−08	1.017e−01	1.636e−01	6.796e−08	6.796e−08	6.796e−08	6.796e−08	6.796e−08	6.796e−08	–
f_3	6.796e−08	6.796e−08	6.796e−08	8.817e−01	3.152e−02	6.796e−08	6.796e−08	6.796e−08	6.796e−08	6.796e−08	9.173e−08	–
f_4	6.796e−08	7.898e−08	6.796e−08	3.648e−01	1.667e−02	4.320e−03	2.596e−05	1.235e−07	7.898e−08	1.431e−07	4.986e−01	–
f_5	7.898e−08	7.353e−01	6.796e−08	1.481e−03	2.390e−01	1.657e−07	3.507e−01	9.278e−05	1.037e−04	5.629e−04	9.045e−03	–
f_6	9.173e−08	7.579e−04	6.796e−08	9.045e−03	3.336e−03	1.600e−05	4.735e−01	8.597e−06	1.481e−03	3.382e−04	3.605e−02	–
f_7	6.796e−08	1.143e−02	6.796e−08	6.040e−03	1.806e−01	3.499e−06	2.390e−02	8.355e−03	1.159e−04	6.610e−05	2.944e−02	–
f_8	6.796e−08	6.796e−08	6.796e−08	1.929e−02	5.609e−01	1.116e−03	3.048e−04	1.431e−07	6.796e−08	6.796e−08	1.136e−01	–
f_9	6.796e−08	6.796e−08	6.796e−08	1.294e−04	3.057e−03	6.796e−08	9.748e−06	6.796e−08	6.796e−08	6.796e−08	5.629e−04	–
f_{10}	6.796e−08	2.218e−07	6.796e−08	7.712e−03	9.045e−03	1.997e−04	2.564e−02	5.227e−07	3.499e−06	6.674e−06	7.205e−03	–

Table 23 The p values between MSICOA and competitor optimizers in 20-D CEC2020

Func	CS	WOA	HGSO	AVOA	AGTO	GJO	HBA	EVO	COA	ICOA	CCOA	MSICOA
f_1	6.796e−08	6.796e−08	6.796e−08	8.357e−04	2.745e−04	6.796e−08	6.796e−08	6.796e−08	6.796e−08	6.796e−08	6.796e−08	–
f_2	6.796e−08	6.796e−08	6.796e−08	4.094e−01	2.799e−03	6.796e−08	6.796e−08	6.796e−08	6.796e−08	6.796e−08	6.796e−08	–
f_3	6.796e−08	6.796e−08	6.796e−08	8.392e−01	6.040e−03	6.796e−08	6.796e−08	6.796e−08	6.796e−08	6.796e−08	6.796e−08	–
f_4	6.796e−08	6.796e−08	6.796e−08	1.014e−03	6.796e−08	6.796e−08	6.796e−08	6.796e−08	6.796e−08	6.796e−08	7.557e−01	–
f_5	6.796e−08	2.616e−01	6.796e−08	6.949e−01	1.436e−02	1.918e−07	5.609e−01	6.917e−07	1.918e−07	6.015e−07	6.750e−01	–
f_6	6.796e−08	2.563e−07	6.796e−08	1.576e−06	2.085e−02	6.796e−08	1.104e−05	6.796e−08	6.796e−08	6.796e−08	7.948e−07	–
f_7	6.796e−08	5.255e−05	6.796e−08	6.949e−01	3.152e−02	6.796e−08	2.287e−01	7.898e−08	6.796e−08	7.898e−08	4.155e−04	–
f_8	6.796e−08	6.796e−08	6.796e−08	2.616e−01	8.355e−03	6.796e−08	6.796e−08	6.796e−08	6.796e−08	6.796e−08	3.382e−04	–
f_9	6.796e−08	6.796e−08	6.796e−08	1.782e−03	6.674e−06	6.796e−08	6.796e−08	6.796e−08	6.796e−08	6.796e−08	9.278e−05	–
f_{10}	6.796e−08	6.796e−08	6.796e−08	5.560e−03	7.113e−03	6.796e−08	1.481e−03	6.796e−08	6.796e−08	6.796e−08	2.341e−03	–

C: Ablation experiments in CEC benchmarks

Tables 24, 25, 26, and 27 summarize the detailed results of ablation experiments in CEC benchmarks, while the p values between COA and its variants are summarized in Tables 28, 29, 30 and 31.

Table 24 Results of ablation experiments in 30-D CEC2017

Func.	COA		COA-NIWF		COA-HHBM		COA-SVM		MSICOA	
	Mean	Std	Mean	Std	Mean	Std	Mean	Std	Mean	Std
f_1	3.166e+10	7.763e+09	1.430e+06 −	3.246e+05	1.375e+06 −	4.491e+05	2.995e+05 −	4.740e+05	**1.096e+04** −	7.515e+03
f_3	8.455e+04	1.084e+04	5.551e+04 −	8.054e+03	5.368e+04 −	7.882e+03	6.446e+04 −	8.502e+03	**3.541e+04** −	5.615e+03
f_4	5.663e+03	1.489e+03	5.333e+02 −	2.503e+01	5.225e+02 −	2.008e+01	5.136e+02 −	2.228e+01	**4.988e+02** −	1.562e+01
f_5	8.333e+02	2.796e+01	6.531e+02 −	2.776e+01	6.691e+02 −	3.370e+01	**6.506e+02** −	3.740e+01	6.998e+02 −	4.687e+01
f_6	6.694e+02	6.950e+00	6.473e+02 −	7.495e+00	6.419e+02 −	6.588e+00	**6.294e+02** −	8.745e+00	6.400e+02 −	1.106e+01
f_7	1.390e+03	5.532e+01	9.795e+02 −	4.122e+01	**9.201e+02** −	2.901e+01	9.686e+02 −	6.513e+01	1.034e+03 −	9.346e+01
f_8	1.102e+03	2.690e+01	**9.125e+02** −	2.305e+01	9.307e+02 −	3.196e+01	9.214e+02 −	3.143e+01	9.478e+02 −	2.855e+01
f_9	8.879e+03	1.642e+03	4.216e+03 −	7.547e+02	3.546e+03 −	7.085e+02	**3.293e+03** −	8.481e+02	5.010e+03 −	9.029e+02
f_{10}	7.907e+03	4.306e+02	5.028e+03 −	3.467e+02	**4.760e+03** −	5.220e+02	6.350e+03 −	9.682e+02	4.927e+03 −	7.181e+02
f_{11}	6.535e+03	1.717e+03	1.351e+03 −	7.725e+01	1.299e+03 −	6.279e+01	**1.279e+03** −	5.387e+01	1.329e+03 −	7.222e+01
f_{12}	2.904e+09	7.865e+08	1.498e+07 −	8.810e+06	1.836e+07 −	1.321e+07	**1.787e+06** −	1.697e+06	1.946e+06 −	2.562e+06
f_{13}	7.977e+08	3.988e+08	1.142e+05 −	4.456e+04	1.175e+05 −	5.428e+04	**2.433e+04** −	2.392e+04	9.574e+04 −	1.684e+05
f_{14}	1.809e+05	2.001e+05	1.718e+05 ≈	1.660e+05	2.760e+05 ≈	3.436e+05	**5.532e+04** −	4.184e+04	6.433e+04 −	5.954e+04
f_{15}	3.602e+06	3.004e+06	3.518e+04 −	1.891e+04	3.413e+04 −	1.267e+04	**4.763e+03** −	4.837e+03	1.848e+04 −	1.276e+04
f_{16}	4.063e+03	2.451e+02	2.907e+03 −	2.023e+02	**2.755e+03** −	2.941e+02	2.881e+03 −	2.607e+02	2.868e+03 −	2.308e+02
f_{17}	2.717e+03	1.596e+02	2.207e+03 −	1.830e+02	**2.130e+03** −	1.377e+02	2.360e+03 −	2.324e+02	2.412e+03 −	2.939e+02
f_{18}	2.230e+06	1.176e+06	4.441e+05 −	5.140e+05	8.034e+05 −	7.567e+05	**2.867e+05** −	1.848e+05	4.002e+05 −	3.471e+05
f_{19}	2.499e+07	2.292e+07	**2.357e+06** −	1.944e+06	1.792e+06 −	1.171e+06	**8.302e+03** −	4.704e+03	1.041e+05 −	3.897e+05
f_{20}	2.803e+03	1.091e+02	**2.455e+03** −	1.288e+02	2.515e+03 −	2.036e+02	2.739e+03 ≈	2.328e+02	2.587e+03 −	2.047e+02
f_{21}	2.625e+03	2.820e+01	**2.421e+03** −	1.654e+01	2.430e+03 −	2.604e+01	2.434e+03 −	4.285e+01	2.457e+03 −	6.974e+01
f_{22}	7.013e+03	1.296e+03	4.402e+03 −	1.922e+03	4.153e+03 −	2.053e+03	6.153e+03 ≈	2.330e+03	**3.337e+03** −	1.805e+03
f_{23}	3.123e+03	7.921e+01	2.889e+03 −	4.659e+01	2.886e+03 −	5.662e+01	**2.850e+03** −	5.583e+01	2.865e+03 −	4.713e+01
f_{24}	3.316e+03	5.408e+01	3.054e+03 −	6.354e+01	3.054e+03 −	5.950e+01	**3.013e+03** −	8.603e+01	3.023e+03 −	8.249e+01
f_{25}	4.485e+03	4.563e+02	2.955e+03 −	2.527e+01	2.943e+03 −	2.699e+01	2.916e+03 −	2.139e+01	**2.888e+03** −	5.720e+00

Table 24 continued

Func.	COA		COA-NIWF		COA-HHBM		COA-SVM		MSICOA	
	Mean	Std	Mean	Std	Mean	Std	Mean	Std	Mean	Std
f_{26}	8.232e+03	7.966e+02	6.485e+03 −	1.505e+03	5.856e+03 −	1.333e+03	**5.265e+03** −	1.359e+03	5.540e+03 −	1.238e+03
f_{27}	3.456e+03	4.998e+01	3.536e+03 +	9.113e+01	3.422e+03 −	7.854e+01	**3.272e+03** −	3.282e+01	3.293e+03 −	9.674e+01
f_{28}	5.410e+03	3.802e+02	3.337e+03 −	3.910e+01	3.304e+03 −	2.502e+01	3.273e+03 −	2.784e+01	**3.228e+03** −	1.624e+01
f_{29}	4.897e+03	3.311e+02	4.406e+03 −	2.178e+02	4.385e+03 −	4.116e+02	4.108e+03 −	2.205e+02	**4.097e+03** −	2.687e+02
f_{30}	1.275e+08	5.837e+07	7.126e+06 −	3.450e+06	6.889e+06 −	2.670e+06	**2.811e+04** −	2.490e+04	1.392e+05 −	3.288e+05
+/≈/−	–		1/1/27		0/1/28		0/2/27		0/0/29	
Avg. rank	4.9		3.2		2.7		**1.9**		2.2	

Table 25 Results of ablation experiments in 50-D CEC2017

Func.	COA		COA-NIWF		COA-HHBM		COA-SVM		MSICOA	
	Mean	Std	Mean	Std	Mean	Std	Mean	Std	Mean	Std
f_1	8.835e+10	1.492e+10	2.368e+08 –	4.391e+08	1.478e+06 –	2.327e+05	1.410e+06 –	1.593e+06	**1.327e+05** –	9.571e+04
f_3	2.097e+05	3.114e+04	1.236e+05 –	9.238e+03	1.211e+05 –	1.789e+04	1.608e+05 –	1.964e+04	**9.971e+04** –	2.633e+04
f_4	2.082e+04	5.009e+03	7.817e+02 –	7.388e+01	6.882e+02 –	5.786e+01	5.947e+02 –	5.555e+01	**5.629e+02** –	5.786e+01
f_5	1.157e+03	4.138e+01	**7.643e+02** –	2.640e+01	7.701e+02 –	3.962e+01	7.715e+02 –	5.042e+01	8.537e+02 –	3.276e+01
f_6	6.899e+02	5.116e+00	6.541e+02 –	4.194e+00	6.555e+02 –	4.171e+00	**6.430e+02** –	5.283e+00	6.518e+02 –	6.059e+00
f_7	2.014e+03	8.664e+01	1.341e+03 –	1.010e+02	**1.227e+03** –	1.085e+02	1.287e+03 –	1.082e+02	1.428e+03 –	1.297e+02
f_8	1.458e+03	3.570e+01	**1.073e+03** –	4.566e+01	1.103e+03 –	5.356e+01	1.095e+03 –	3.413e+01	1.167e+03 –	5.154e+01
f_9	3.119e+04	2.534e+03	1.284e+04 –	1.713e+03	1.198e+04 –	2.251e+03	1.217e+04 –	4.018e+03	**1.176e+04** –	1.278e+03
f_{10}	1.408e+04	7.037e+02	7.492e+03 –	6.587e+02	**7.460e+03** –	7.714e+02	8.641e+03 –	8.810e+02	7.829e+03 –	9.960e+02
f_{11}	1.687e+04	4.076e+03	3.218e+03 –	7.744e+02	1.871e+03 –	2.586e+02	1.414e+03 –	6.525e+01	**1.413e+03** –	8.628e+01
f_{12}	2.116e+10	6.194e+09	4.394e+07 –	1.807e+07	6.124e+07 –	3.900e+07	1.117e+07 –	6.999e+06	**9.340e+06** –	6.588e+06
f_{13}	6.874e+09	2.328e+09	1.669e+05 –	4.873e+04	1.676e+05 –	4.912e+04	**1.804e+04** –	9.706e+03	1.041e+05 –	5.998e+04
f_{14}	3.219e+06	2.299e+06	3.694e+05 –	3.346e+05	4.066e+05 –	2.192e+05	4.537e+05 –	2.928e+05	**2.441e+05** –	1.863e+05
f_{15}	5.975e+08	4.390e+08	6.096e+04 –	1.352e+04	5.766e+04 –	2.808e+04	**1.484e+04** –	9.312e+03	6.597e+04 –	6.001e+04
f_{16}	6.387e+03	3.996e+02	3.642e+03 –	3.800e+02	3.746e+03 –	4.350e+02	**3.500e+03** –	5.525e+02	3.615e+03 –	4.792e+02
f_{17}	4.735e+03	4.512e+02	3.169e+03 –	2.930e+02	**3.084e+03** –	3.476e+02	3.486e+03 –	3.597e+02	3.574e+03 –	3.505e+02
f_{18}	1.785e+07	1.380e+07	2.610e+06 –	2.427e+06	1.809e+06 –	1.258e+06	1.866e+06 –	1.067e+06	**8.571e+05** –	4.654e+05
f_{19}	3.957e+08	1.565e+08	2.242e+06 –	2.049e+06	2.142e+06 –	2.077e+06	**1.760e+04** –	8.825e+03	1.154e+05 –	1.672e+05
f_{20}	3.808e+03	2.433e+02	3.016e+03 –	1.818e+02	**2.922e+03** –	2.652e+02	3.301e+03 –	2.701e+02	3.203e+03 –	2.660e+02
f_{21}	3.003e+03	4.458e+01	**2.576e+03** –	3.850e+01	2.582e+03 –	5.570e+01	2.592e+03 –	6.978e+01	2.673e+03 –	7.621e+01
f_{22}	1.571e+04	6.130e+02	9.633e+03 –	8.775e+02	**9.546e+03** –	8.122e+02	1.047e+04 –	9.190e+02	9.587e+03 –	2.080e+03
f_{23}	3.865e+03	1.110e+02	3.387e+03 –	1.415e+02	3.336e+03 –	1.452e+02	3.240e+03 –	1.446e+02	**3.200e+03** –	1.251e+02
f_{24}	4.081e+03	1.999e+02	3.624e+03 –	8.797e+01	3.476e+03 –	1.348e+02	3.347e+03 –	9.818e+01	**3.341e+03** –	1.849e+02

Table 25 continued

Func.	COA		COA-NIWF		COA-HHBM		COA-SVM		MSICOA	
	Mean	Std	Mean	Std	Mean	Std	Mean	Std	Mean	Std
f_{25}	1.304e+04	1.881e+03	3.306e+03 −	7.053e+01	3.201e+03 −	4.017e+01	3.131e+03 −	3.568e+01	**3.090e+03** −	2.374e+01
f_{26}	1.445e+04	1.207e+03	1.141e+04 −	9.111e+02	1.047e+04 −	1.431e+03	8.788e+03 −	2.515e+03	**6.770e+03** −	3.544e+03
f_{27}	4.512e+03	1.786e+02	4.681e+03 +	1.867e+02	4.524e+03 ≈	3.536e+02	3.794e+03 −	2.096e+02	**3.557e+03** −	1.213e+02
f_{28}	1.012e+04	9.090e+02	4.047e+03 −	2.295e+02	3.800e+03 −	1.645e+02	3.415e+03 −	3.815e+01	**3.345e+03** −	3.383e+01
f_{29}	9.060e+03	1.072e+03	6.259e+03 −	5.620e+02	5.921e+03 −	5.190e+02	**4.938e+03** −	2.493e+02	4.978e+03 −	3.968e+02
f_{30}	1.209e+09	4.942e+08	1.150e+08 −	1.848e+07	1.026e+08 −	1.555e+07	**1.717e+06** −	7.130e+05	3.598e+06 −	1.720e+06
+/≈/−	–		1/0/28		0/1/28		0/0/29		0/0/29	
Avg. rank	4.9		3.2		2.6		2.3		**2.0**	

Table 26 Results of ablation experiments in 10-D CEC2020

Func.	COA		COA-NIWF		COA-HHBM		COA-SVM		MSICOA	
	Mean	Std	Mean	Std	Mean	Std	Mean	Std	Mean	Std
f_1	1.346e+09	6.476e+08	7.018e+05 −	3.143e+05	4.662e+05 −	1.987e+05	3.021e+03 −	3.157e+03	**2.815e+03** −	2.465e+03
f_2	1.200e+11	7.056e+10	5.366e+07 −	3.276e+07	4.564e+07 −	2.340e+07	**2.822e+05** −	3.052e+05	5.671e+05 −	4.521e+05
f_3	4.156e+10	1.636e+10	1.999e+07 −	1.001e+07	1.551e+07 −	7.363e+06	**6.161e+04** −	7.823e+04	2.076e+05 −	2.281e+05
f_4	2.000e+03	2.109e+02	1.902e+03 −	8.734e−01	**1.902e+03** −	9.783e−01	1.902e+03 −	8.330e−01	1.903e+03 −	2.037e+00
f_5	4.340e+04	2.497e+04	4.675e+04 ≈	3.019e+04	5.483e+04 ≈	3.525e+04	1.438e+04 −	8.856e+03	**1.377e+04** −	1.125e+04
f_6	3.748e+03	1.551e+03	4.147e+03 ≈	1.883e+03	3.596e+03 ≈	1.825e+03	3.794e+03 ≈	3.531e+03	**2.686e+03** −	1.582e+03
f_7	4.503e+04	3.400e+04	1.701e+04 −	8.619e+03	1.711e+04 −	8.799e+03	**1.280e+04** −	8.703e+03	1.492e+04 −	1.481e+04
f_8	2.321e+03	4.258e+00	2.305e+03 −	1.768e+00	**2.304e+03** −	1.891e+00	2.305e+03 −	1.926e+00	2.305e+03 −	2.345e+00
f_9	4.240e+03	3.104e+02	2.600e+03 −	5.022e+01	2.596e+03 −	5.849e+01	2.578e+03 −	5.931e+01	**2.560e+03** −	4.899e+01
f_{10}	3.076e+03	3.813e+01	3.039e+03 −	4.585e+01	3.043e+03 ≈	5.059e+01	3.013e+03 −	3.953e+01	**2.999e+03** −	3.462e+01
+/≈/−	–		0/2/8		0/3/7		0/1/9		0/0/10	
Avg. rank	4.6		3.6		2.9		2.1		**1.8**	

Table 27 Results of ablation experiments in 20-D CEC2020

Func.	COA		COA-NIWF		COA-HHBM		COA-SVM		MSICOA	
	Mean	Std	Mean	Std	Mean	Std	Mean	Std	Mean	Std
f_1	9.330e+09	2.370e+09	7.969e+05–	2.125e+05	7.473e+05–	2.490e+05	1.509e+04–	2.180e+04	**6.325e+03**–	4.129e+03
f_2	1.110e+12	3.645e+11	7.765e+07	2.556e+07	6.800e+07–	2.242e+07	1.526e+06–	2.913e+06	**7.174e+05**–	7.290e+05
f_3	3.236e+11	8.843e+10	2.801e+07–	1.070e+07	2.675e+07–	8.185e+06	5.083e+05–	6.612e+05	**3.366e+05**–	3.599e+05
f_4	7.457e+03	6.440e+03	1.916e+03–	3.293e+00	1.911e+03–	3.521e+00	1.912e+03–	6.162e+00	**1.906e+03**–	1.580e+00
f_5	2.958e+06	1.548e+06	1.004e+06–	9.245e+05	9.535e+05–	7.125e+05	**3.164e+05**–	2.481e+05	3.627e+05–	4.521e+05
f_6	7.735e+04	4.484e+04	2.231e+04–	7.264e+03	1.241e+04–	6.272e+03	5.633e+03–	3.731e+03	**2.951e+03**–	1.101e+03
f_7	3.139e+06	2.545e+06	1.794e+05–	2.155e+05	1.770e+05–	1.436e+05	**1.523e+04**–	7.417e+03	3.520e+04–	6.211e+04
f_8	2.458e+03	3.541e+01	2.363e+03–	1.423e+01	2.349e+03–	1.347e+01	2.338e+03–	7.667e+00	**2.334e+03**–	2.833e+00
f_9	1.043e+04	1.736e+03	2.692e+03–	6.753e+01	2.668e+03–	4.116e+01	2.661e+03–	1.116e+02	**2.618e+03**–	7.488e+01
f_{10}	4.549e+03	4.557e+02	3.584e+03–	1.825e+02	3.500e+03–	1.529e+02	3.295e+03–	8.020e+01	**3.200e+03**–	5.829e+01
+/≈/−	–		0/0/10		0/0/10		0/0/10		0/0/10	
Avg. rank	5.0		4.0		2.9		1.9		**1.2**	

Table 28 The p values between COA and its variants in 30-D CEC2017

Func	COA	COA-NIWF	COA-HHBM	COA-SVM	MSICOA
f_1	–	6.796e−08	6.796e−08	6.796e−08	6.796e−08
f_3	–	6.917e−07	3.939e−07	5.874e−06	6.796e−08
f_4	–	6.796e−08	6.796e−08	6.796e−08	6.796e−08
f_5	–	6.796e−08	6.796e−08	6.796e−08	1.065e−07
f_6	–	1.657e−07	9.173e−08	6.796e−08	1.065e−07
f_7	–	6.796e−08	6.796e−08	6.796e−08	6.796e−08
f_8	–	6.796e−08	6.796e−08	6.796e−08	6.796e−08
f_9	–	9.173e−08	6.796e−08	6.796e−08	2.218e−07
f_{10}	–	6.796e−08	6.796e−08	5.874e−06	6.796e−08
f_{11}	–	6.796e−08	6.796e−08	6.796e−08	6.796e−08
f_{12}	–	6.796e−08	6.796e−08	6.796e−08	6.796e−08
f_{13}	–	6.796e−08	6.796e−08	6.796e−08	6.796e−08
f_{14}	-	1.000e+00	8.817e−01	3.639e−03	1.929e−02
f_{15}	–	6.796e−08	6.796e−08	6.796e−08	6.796e−08
f_{16}	–	6.796e−08	6.796e−08	6.796e−08	6.796e−08
f_{17}	–	2.218e−07	9.173e−08	2.041e−05	1.349e−03
f_{18}	–	5.874e−06	8.292e−05	2.218e−07	6.917e−07
f_{19}	–	3.499e−06	2.690e−06	6.796e−08	7.898e−08
f_{20}	–	4.539e−07	1.600e−05	1.075e−01	9.278e−05
f_{21}	–	6.796e−08	6.796e−08	6.796e−08	6.796e−08
f_{22}	–	5.091e−04	2.745e−04	8.181e−01	9.748e−06
f_{23}	–	1.065e−07	1.657e−07	1.065e−07	1.065e−07
f_{24}	–	7.898e−08	7.898e−08	1.065e−07	2.563e−07
f_{25}	–	6.796e−08	6.796e−08	6.796e−08	6.796e−08
f_{26}	–	1.600e−05	6.015e−07	9.173e−08	1.431e−07
f_{27}	–	2.799e−03	1.667e−02	7.898e−08	9.748e−06
f_{28}	–	6.796e−08	6.796e−08	6.796e−08	6.796e−08
f_{29}	–	2.925e−05	5.091e−04	2.563e−07	2.960e−07
f_{30}	–	6.796e−08	6.796e−08	6.796e−08	6.796e−08

Table 29 The p values between COA and its variants in 50-D CEC2017

Func	COA	COA-NIWF	COA-HHBM	COA-SVM	MSICOA
f_1	–	6.796e−08	6.796e−08	6.796e−08	6.796e−08
f_3	–	6.796e−08	6.796e−08	8.597e−06	6.796e−08
f_4	–	6.796e−08	6.796e−08	6.796e−08	6.796e−08
f_5	–	6.796e−08	6.796e−08	6.796e−08	6.796e−08
f_6	–	6.796e−08	6.796e−08	6.796e−08	6.796e−08
f_7	–	6.796e−08	6.796e−08	6.796e−08	6.796e−08
f_8	–	6.796e−08	6.796e−08	6.796e−08	6.796e−08
f_9	–	6.796e−08	6.796e−08	6.796e−08	6.796e−08
f_{10}	–	6.796e−08	6.796e−08	6.796e−08	6.796e−08
f_{11}	–	6.796e−08	6.796e−08	6.796e−08	6.796e−08
f_{12}	–	6.796e−08	6.796e−08	6.796e−08	6.796e−08
f_{13}	–	6.796e−08	6.796e−08	6.796e−08	6.796e−08
f_{14}	–	1.918e−07	6.796e−08	9.173e−08	6.796e−08
f_{15}	–	6.796e−08	6.796e−08	6.796e−08	6.796e−08
f_{16}	–	6.796e−08	6.796e−08	6.796e−08	6.796e−08
f_{17}	–	6.796e−08	6.796e−08	1.431e−07	1.657e−07
f_{18}	–	5.227e−07	1.235e−07	1.065e−07	6.796e−08
f_{19}	–	6.796e−08	6.796e−08	6.796e−08	6.796e−08
f_{20}	–	9.173e−08	7.898e−08	6.674e−06	1.201e−06
f_{21}	–	6.796e−08	6.796e−08	6.796e−08	6.796e−08
f_{22}	–	6.796e−08	6.796e−08	6.796e−08	6.796e−08
f_{23}	–	7.898e−08	6.796e−08	6.796e−08	6.796e−08
f_{24}	–	6.796e−08	6.796e−08	6.796e−08	1.235e−07
f_{25}	–	6.796e−08	6.796e−08	6.796e−08	6.796e−08
f_{26}	–	1.431e−07	1.065e−07	6.796e−08	6.796e−08
f_{27}	–	1.234e−02	8.181e−01	1.065e−07	6.796e−08
f_{28}	–	6.796e−08	6.796e−08	6.796e−08	6.796e−08
f_{29}	–	1.065e−07	6.796e−08	6.796e−08	6.796e−08
f_{30}	–	6.796e−08	6.796e−08	6.796e−08	6.796e−08

Table 30 The p values between COA and its variants in 10-D CEC2020

Func	COA	COA-NIWF	COA-HHBM	COA-SVM	MSICOA
f_1	–	6.796e−08	6.796e−08	6.796e−08	6.796e−08
f_2	–	6.796e−08	6.796e−08	6.796e−08	6.796e−08
f_3	–	6.796e−08	6.796e−08	6.796e−08	6.796e−08
f_4	–	6.796e−08	6.796e−08	6.796e−08	7.898e−08
f_5	–	1.000e+00	4.570e−01	8.292e−05	1.037e−04
f_6	–	5.250e−01	4.407e−01	5.310e−02	1.481e−03
f_7	–	3.750e−04	8.357e−04	4.680e−05	1.159e−04
f_8	–	6.796e−08	6.796e−08	6.796e−08	6.796e−08
f_9	–	6.796e−08	6.796e−08	6.796e−08	6.796e−08
f_{10}	–	5.115e−03	5.310e−02	2.596e−05	3.499e−06

Table 31 The p values between COA and its variants in 20-D CEC2020

Func	COA	COA-NIWF	COA-HHBM	COA-SVM	MSICOA
f_1	–	6.796e−08	6.796e−08	6.796e−08	6.796e−08
f_2	–	6.796e−08	6.796e−08	6.796e−08	6.796e−08
f_3	–	6.796e−08	6.796e−08	6.796e−08	6.796e−08
f_4	–	6.796e−08	6.796e−08	6.796e−08	6.796e−08
f_5	–	3.293e−05	1.104e−05	6.796e−08	1.918e−07
f_6	–	2.356e−06	1.431e−07	6.796e−08	6.796e−08
f_7	–	1.235e−07	7.898e−08	6.796e−08	6.796e−08
f_8	–	6.796e−08	6.796e−08	6.796e−08	6.796e−08
f_9	–	6.796e−08	6.796e−08	6.796e−08	6.796e−08
f_{10}	–	3.416e−07	1.065e−07	6.796e−08	6.796e−08

Acknowledgements This work was supported by the basic ability enhancement programs for Young and Middle-Aged Teachers of Guangxi 2022KY0767 and 2024KY0787 and the Scientific Research Foundation of Guangxi Minzu Normal University 2024YB122.

Author contribution Chunqing Li: contributed to conceptualization, methodology, investigation, writing—original draft, writing—review and editing, and funding acquisition. Zhongmin Wang: involved in resources, data curation, and writing—review and editing. Jun Yu: contributed to resources and writing—review and editing. Mahmoud Abdel-Salam: involved in resources and writing—review and editing. Essam H. Houssein: contributed to investigation and writing—review and editing. Rui Zhong: provided software and was involved in writing—original draft, writing—review and editing, supervision, and project administration.

Data availability The source code of this research can be downloaded at https://github.com/RuiZhong961230/MSICOA.

Declarations

Conflict of interest The authors declare no conflict of interest.

References

1. Rajwar K, Deep K, Das S (2023) An exhaustive review of the metaheuristic algorithms for search and optimization: taxonomy, applications, and open challenges. Artif Intell Rev 56(11):13187–13257
2. Lian J, Hui G (2023) Human evolutionary optimization algorithm. Expert Syst Appl 241:1
3. Lian J, Hui G, Ma L, Zhu T, Wu X, Heidari AA, Chen Y, Chen H (2024) Parrot optimizer: algorithm and applications to medical problems (ESI hot paper). Comput Biol Med 172:108064
4. Gharehchopogh FS (2023) Quantum-inspired metaheuristic algorithms: comprehensive survey and classification. Artif Intell Rev 56(6):5479–5543
5. Zhong R, Yu J (2024) Gene-targeting multiplayer battle game optimizer for large-scale global optimization via cooperative coevolution. Clust Comput 27:12483–12508
6. Zhang Y-J, Wang Y-F, Yan Y, Zhao J, Gao Z-M (2024) Historical knowledge transfer driven self-adaptive evolutionary multitasking algorithm with hybrid resource release for solving nonlinear equation systems. Swarm Evol Comput 91:101754
7. Nayak J, Swapnarekha H, Naik B, Dhiman G, Vimal S (2023) 25 years of particle swarm optimization: flourishing voyage of two decades. Arch Comput Methods Eng 30(3):1663–1725
8. Awadallah MA, Makhadmeh SN, Al-Betar MA, Dalbah LM, Al-Redhaei A, Kouka S, Enshassi OS (2024) Multi-objective ant colony optimization. Arch Comput Methods Eng 1:1–43
9. Londe MA, Pessoa LS, Andrade CE, Resende MGC (2025) Biased random-key genetic algorithms: a review. Eur J Oper Res 321(1):1–22
10. Dehghani M, Trojovskỳ P (2023) Osprey optimization algorithm: a new bio-inspired metaheuristic algorithm for solving engineering optimization problems. Front Mech Eng 8:1126450
11. Trojovskỳ P, Dehghani M (2022) Pelican optimization algorithm: a novel nature-inspired algorithm for engineering applications. Sensors 22(3):855
12. Abdollahzadeh B, Soleimanian Gharehchopogh F, Mirjalili S (2021) Artificial gorilla troops optimizer: a new nature-inspired metaheuristic algorithm for global optimization problems. Int J Intell Syst 36(10):5887–5958
13. Xue J, Shen B (2023) Dung beetle optimizer: a new meta-heuristic algorithm for global optimization. J Supercomput 79(7):7305–7336
14. Zhong R, Yu J, Zhang C, Munetomo M (2024) Srime: a strengthened rime with latin hypercube sampling and embedded distance-based selection for engineering optimization problems. Neural Comput Appl 36:6721–6740
15. Xue Y, Zhu A (2024) An effective surrogate-assisted rank method for evolutionary neural architecture search. Appl Soft Comput 167:112392
16. Wu F, Li S, Zhang J, Xie R, Yang M (2024) Bernstein-based oppositional-multiple learning and differential enhanced exponential distribution optimizer for real-world optimization problems. Eng Appl Artif Intell 138:109370
17. Zhang Y-J, Wang Y-F, Yan Y-X, Zhao J, Gao Z-M (2024) Self-adaptive hybrid mutation slime mould algorithm: case studies on UAV path planning, engineering problems, photovoltaic models and infinite impulse response. Alex Eng J 98:364–389
18. Zhong R, Zhang C, Yu J (2025) Hierarchical rime algorithm with multiple search preferences for extreme learning machine training. Alex Eng J 110:77–98
19. Han M, Du Z, Yuen KF, Zhu H, Li Y, Yuan Q (2024) Walrus optimizer: a novel nature-inspired metaheuristic algorithm. Expert Syst Appl 239:122413
20. Wang W-C, Tian W-C, Xu D-M, Zang H-F (2024) Arctic puffin optimization: a bio-inspired metaheuristic algorithm for solving engineering design optimization. Adv Eng Softw 195:103694
21. Sowmya R, Premkumar M, Jangir P (2024) Newton–Raphson-based optimizer: a new population-based metaheuristic algorithm for continuous optimization problems. Eng Appl Artif Intell 128:107532
22. Xu Y, Zhong R, Zhang C, Yu J (2025) Crested ibis algorithm and its application in human-powered aircraft design. Knowl Based Syst 310:113020
23. Dehghani M, Montazeri Z, Trojovská E, Trojovský P (2023) Coati optimization algorithm: a new bio-inspired metaheuristic algorithm for solving optimization problems. Knowl Based Syst 259:110011
24. Abdollahzadeh B, Khodadadi N, Barshandeh S, Trojovskỳ P, Gharehchopogh FS, El-kenawy ESM, Abualigah L, Mirjalili S (2024) Puma optimizer (PO): a novel metaheuristic optimization algorithm and its application in machine learning. Clust Comput 1:1–49
25. Alqudah NE, Abed-alguni B, Barhoush M (2024) Bi-objective feature selection in high-dimensional datasets using improved binary chimp optimization algorithm. Int J Mach Learn Cybern 15:6107–6148
26. Abed-alguni B, Mohammad B, Alawad NA (2024) BOC-PDO: an intrusion detection model using binary opposition cellular prairie dog optimization algorithm. Clust Comput 27:14417–14449

27. Qi Z, Yingjie D, Shan Y, Xu L, Dongcheng H, Guoqi X (2024) An improved coati optimization algorithm with multiple strategies for engineering design optimization problems. Sci Rep 14:1
28. Houssein EH, Samee NA, Mahmoud NF, Hussain K (2023) Dynamic coati optimization algorithm for biomedical classification tasks. Comput Biol Med 164:107237
29. Hashim FA, Houssein EH, Mostafa RR, Hussien AG, Helmy F (2023) An efficient adaptive-mutated coati optimization algorithm for feature selection and global optimization. Alex Eng J 85:29–48
30. Hasanien HM, Alsaleh I, Alassaf A, Alateeq A (2023) Enhanced coati optimization algorithm-based optimal power flow including renewable energy uncertainties and electric vehicles. Energy 283:129069
31. Raj S, Bharti RK, Tripathi K (2024) Coati optimization algorithm based deep convolutional forest method for prediction of atmospheric and oceanic parameters. Sci Rep 14(1):22160
32. Houssein EH, Hammad A, Emam MM, Ali AA (2024) An enhanced coati optimization algorithm for global optimization and feature selection in EEG emotion recognition. Comput Biol Med 173:108329
33. Miao F, Li H, Mei X (2024) Three-dimensional path planning of UAVS for offshore rescue based on a modified coati optimization algorithm. J Mar Sci Eng 12(9):1
34. Heidari AA, Mirjalili S, Faris H, Aljarah I, Mafarja M, Chen H (2019) Harris hawks optimization: algorithm and applications. Futur Gener Comput Syst 97:849–872
35. Xue J, Shen B (2020) A novel swarm intelligence optimization approach: sparrow search algorithm. Syst Sci Control Eng 8(1):22–34
36. Wu X, Ding Y, Wang L, Zhang H (2025) A multi-strategy adaptive coati optimization Algorithm for constrained optimization engineering design problems. Biomimetics 10:323. https://doi.org/10.3390/biomimetics10050323
37. Wu G, Mallipeddi R, Suganthan PN (2017) Problem definitions and evaluation criteria for the CEC 2017 competition on constrained real-parameter optimization. National University of Defense Technology, Changsha, Hunan, PR China and Kyungpook National University, Daegu, South Korea and Nanyang Technological University, Singapore, Technical Report
38. Yue D, Price K, PSLJ, Ali M, Qu B (2019) Problem definitions and evaluation criteria for CEC 2020 competition on single objective bound constrained numerical optimization. Zhengzhou University (China), Nanyang Technological University (Singapore)
39. Van Thieu N (2024) Opfunu: an open-source python library for optimization benchmark functions. J Open Res Softw 1:1
40. Yang X-S, Deb S (2009) Cuckoo search via lévy flights. In: 2009 World congress on nature and biologically inspired computing (NaBIC), pp 210–214
41. Mirjalili S, Lewis A (2016) The whale optimization algorithm. Adv Eng Softw 95:51–67
42. Hashim FA, Houssein EH, Mabrouk MS, Al-Atabany W, Mirjalili S (2019) Henry gas solubility optimization: a novel physics-based algorithm. Futur Gener Comput Syst 101:646–667
43. Abdollahzadeh B, Gharehchopogh FS, Mirjalili S (2021) African vultures optimization algorithm: a new nature-inspired metaheuristic algorithm for global optimization problems. Comput Ind Eng 158:107408
44. Chopra N, Mohsin Ansari M (2022) Golden jackal optimization: a novel nature-inspired optimizer for engineering applications. Expert Syst Appl 198:116924
45. Hashim FA, Houssein EH, Hussain K, Mabrouk MS, Al-Atabany W (2022) Honey badger algorithm: new metaheuristic algorithm for solving optimization problems. Math Comput Simul 192:84–110
46. Azizi M, Aickelin U, Khorshidi H, Baghalzadeh Shishehgarkhaneh M (2023) Energy valley optimizer: a novel metaheuristic algorithm for global and engineering optimization. Sci Rep 13:226
47. Jia H, Shi S, Wu D, Rao H, Zhang J, Abualigah L (2023) Improve coati optimization algorithm for solving constrained engineering optimization problems. J Comput Des Eng 10(6):2223–2250
48. Zhong R, Zhang C, Yu J (2024) Cooperative coati optimization algorithm with transfer functions for feature selection and knapsack problems. Knowl Inf Syst 66:6933–6974
49. Van Thieu N, Mirjalili S (2023) Mealpy: an open-source library for latest meta-heuristic algorithms in python. J Syst Architect 139:102871
50. Li K, Huang H, Fu S, Ma C, Fan Q, Zhu Y (2023) A multi-strategy enhanced northern goshawk optimization algorithm for global optimization and engineering design problems. Comput Methods Appl Mech Eng 415:116199
51. Bayzidi H, Talatahari S, Saraee M, Lamarche C-P (2021) Social network search for solving engineering optimization problems. Comput Intell Neurosci 2021(1):8548639
52. Thieu NV (2023) ENOPPY: a python library for engineering optimization problems. Zenodo
53. Xu C, Liu Q, Huang T (2022) Resilient penalty function method for distributed constrained optimization under byzantine attack. Inf Sci 596:362–379

Chunqing Li holds a Master of Engineering (M.Eng.) degree from Guangxi University and is currently an Associate Professor at Guangxi MinZu Normal University. Her primary research focuses on intelligent optimization algorithms, data mining, and recommendation systems. She has led and completed multiple municipal- and departmental-level research projects and has published eight high-quality academic papers in related fields.

Zhongmin Wang received the M.S. degree in computer science from Guangxi University for Nationalities in 2021. Currently serving as an assistant lecturer at Yunnan Agricultural University. His research interests are in the areas of computation intelligence and intelligence information systems.

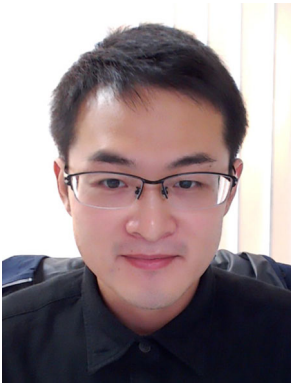

Jun Yu received a Bachelor degree from Northeastern University, China in 2014, and a Master degree and a doctorate from Kyushu University, Japan in 2017 and 2019, respectively. He is currently an Assistant Professor at Niigata University, Japan. His research interests include evolutionary computation, artificial neural networks, and machine learning.

Mahmoud Abdel-Salam has demonstrated exceptional expertise through numerous research contributions in high-impact journals and leading international conferences indexed by Clarivate Analytics JCR, Scopus, Web of Science, and other prestigious scientific platforms. His work also includes book chapters published by Springer and Procedia Computer Science. He serves as a regular reviewer for internationally recognized journals with high-impact factors indexed by Clarivate Analytics and Web of Science. His research interests span a diverse range of topics, including web technologies, cybersecurity, artificial intelligence, optimization problems, evolutionary algorithms, web service composition, big data analytics, data mining, and cloud computing.

Essam H. Houssein (Member, IEEE) received Ph.D. degree in computer science, in 2012. He is currently a Professor of Artificial Intelligence at the Faculty of Computers and Information, Minia University, Minia, Egypt. He is the founder and chair of the Artificial Intelligence Research (AIR) Group, Egypt. He is selected as a Highly Cited Researcher 2023, in 2024 Edition of the Ranking of Top Scientists in the field of Computer Science. He has published more than 240 scientific research articles in prestigious international journals. His research interests include Meta-heuristics Optimization Algorithms, Artificial Intelligence, WSN, Bioinformatics, Internet of Things, Artificial Intelligence, Image Processing, and Data Mining. He serves as a reviewer for more than 120 journals, such as Elsevier, Springer, and IEEE.

Rui Zhong received the B. Eng. degree from Huazhong Agricultural University, China, in 2019, the M. Eng. degree from Kyushu University, Japan, in 2022, and a Ph.D. from Hokkaido University, Japan, in 2024. He is now a Specifically Appointed Assistant Professor at the Information Initiative Center, Hokkaido University. He has published more than 50 articles in high-reputation journals. His research interests include computational intelligence, evolutionary computation, large-scale optimization, meta-/hyper-heuristics, and real-world applications. His profile in Google Scholar can be found at https://scholar.google.com/citations?hl=en&user=xd1vrwIAAAAJ\&view_op=list_works\&sortby=pubdate.

Authors and Affiliations

Chunqing Li[1] · Zhongmin Wang[2] · Jun Yu[3] · Mahmoud Abdel-Salam[4] · Essam H. Houssein[5,6] · Rui Zhong[7]

✉ Rui Zhong
zhongrui@iic.hokudai.ac.jp

Chunqing Li
lichunqing@gxnun.edu.cn

Zhongmin Wang
zhongminwang@ynau.edu.cn

Jun Yu
yujun@ie.niigata-u.ac.jp

Mahmoud Abdel-Salam
mahmoud20@mans.edu.eg

Essam H. Houssein
essam.halim@mu.edu.eg

1 College of Mathematics and Computer Science, Guangxi Minzu Normal University, Chongzuo, China

2 College of Tropical Crops, Yunnan Agricultural University, Yunnan, China

3 Institute of Science and Technology, Niigata University, Niigata, Japan

4 Faculty of Computer and Information Science, Mansoura University, Mansoura, Egypt

5 Faculty of Computers and Information, Minia University, Minia, Egypt

6 Minia National University, Minia, Egypt

7 Information Initiative Center, Hokkaido University, Sapporo, Japan